

RESEARCH ARTICLE

Notch signaling is a novel regulator of visceral smooth muscle cell differentiation in the murine ureter

Jennifer Kurz^{1,*}, Anna-Carina Weiss^{1,*}, Hauke Thiesler², Fairouz Qasrawi¹, Lena Deuper¹, Jaskiran Kaur¹, Carsten Rudat¹, Timo H. Lüdtkke¹, Irina Wojahn¹, Herbert Hildebrandt², Mark-Oliver Trowe¹ and Andreas Kispert^{1,‡}

ABSTRACT

The contractile phenotype of smooth muscle cells (SMCs) is transcriptionally controlled by a complex of the DNA-binding protein SRF and the transcriptional co-activator MYOCD. The pathways that activate expression of *Myocd* and of SMC structural genes in mesenchymal progenitors are diverse, reflecting different intrinsic and extrinsic signaling inputs. Taking the ureter as a model, we analyzed whether Notch signaling, a pathway previously implicated in vascular SMC development, also affects visceral SMC differentiation. We show that mice with a conditional deletion of the unique Notch mediator RBPJ in the undifferentiated ureteric mesenchyme exhibit altered ureter peristalsis with a delayed onset, and decreased contraction frequency and intensity at fetal stages. They also develop hydroureter 2 weeks after birth. Notch signaling is required for precise temporal activation of *Myocd* expression and, independently, for expression of a group of late SMC structural genes. Based on additional expression analyses, we suggest that a mesenchymal JAG1-NOTCH2/NOTCH3 module regulates visceral SMC differentiation in the ureter in a biphasic and bimodal manner, and that its molecular function differs from that in the vascular system.

KEY WORDS: Ureter, Smooth muscle, Rbpj, Notch, Myocd

INTRODUCTION

Smooth muscle cells (SMCs) are found in the mesenchymal wall of many visceral tubular organs but also as an ensheathment of endothelial cells in the vascular system. Owing to their contractile activity, they play a decisive role in maintaining the flexibility and rigidity of these tubes, and in mediating the unidirectional transport of their luminal content. SMCs arise from a diverse range of progenitors and show a high phenotypic plasticity, yet their specialized contractile phenotype seems universally transcriptionally controlled by a complex of the DNA-binding protein serum response factor (SRF) and the co-activator myocardin (MYOCD) (Norman et al., 1988; Wang and Olson, 2004; Yoshida et al., 2003). Expression of *Myocd* and of SMC structural genes occurs in SMC progenitors as a response to a multitude of extrinsic and intrinsic signals. The nature of these signals seems fundamentally different in

vascular and visceral SMC progenitors, probably owing to their specific association with endothelial and epithelial primordia, respectively (Creemers et al., 2006; Donadon and Santoro, 2021; Mack, 2011; Shi and Chen, 2016).

Owing to its simple design, its pharmacological and genetic accessibility, and its relevance for congenital anomalies in humans, the murine ureter is an attractive model with which to unravel the regulatory network that drives visceral SMC differentiation during organogenesis (Bohnenpoll and Kispert, 2014; Woolf and Davies, 2013; Woolf et al., 2019). Previous work has shown that visceral SMCs of the mouse ureter arise at embryonic day (E)11.0 from a *Tbx18*⁺ mesenchymal progenitor pool that surrounds the distal aspect of the ureteric bud: an epithelial diverticulum of the nephric duct (Bohnenpoll et al., 2013). Until E14.5, two signals from the ureteric epithelium (UE), SHH and WNTs, act on the undifferentiated ureteric mesenchyme (UM) to maintain its proliferative expansion and trigger SMC differentiation. SHH activates the expression of the transcription factor gene *Foxf1* in the UM, which, in turn, induces and synergizes with the signaling molecule BMP4 in activation of *Myocd* and SMC structural genes (Bohnenpoll et al., 2017c; Mamo et al., 2017; Yu et al., 2002). WNTs act, at least partly, through the transcription factors TBX2 and TBX3 to maintain BMP4 signaling and suppress an outer adventitial fate (Aydogdu et al., 2018; Trowe et al., 2012). Retinoic acid (RA) synthesized in both the UM and UE inhibits SMC differentiation possibly by counteracting WNT signaling (Bohnenpoll et al., 2017b). As a consequence of a poorly understood interplay of these and most likely additional signals, *Myocd* is precisely activated in the inner layer of the proximal UM at E14.5, expression of SMC structural genes starts at E15.5, and a peristaltically active SMC layer is established concomitantly with the onset of urine production in the kidney around E16.5 (Bohnenpoll et al., 2017a).


Notch signaling is an evolutionarily conserved pathway that mediates contact-dependent cell-to-cell communication in a variety of developmental contexts. In mammals, four Notch receptors (NOTCH1-4) and five ligands [jagged 1 (JAG1), jagged 2 (JAG2), delta-like 1 (DLL1), delta-like 3 (DLL3) and delta-like 4 (DLL4)] are described, which are all type I transmembrane proteins. Ligand-receptor interaction triggers proteolytic cleavages that release the intracellular domain of the receptor (NICD) from the membrane. NICD translocates to the nucleus where it forms an active transcriptional complex with the transcription factor RBPJ and several co-activators (Henrique and Schweisguth, 2019; Kopan, 2012; Kovall et al., 2017). Notch signaling has been characterized as a crucial pathway for vascular SMC differentiation (Baeten and Lilly, 2017; Fouillade et al., 2012), whereas its potential role in visceral SMC development has remained unexplored.

¹Institute of Molecular Biology, Medizinische Hochschule Hannover, 30625

Hannover, Germany. ²Institute of Clinical Biochemistry, Medizinische Hochschule Hannover, 30625 Hannover, Germany.

*These authors contributed equally to this work

‡Author for correspondence (kispert.andreas@mh-hannover.de)

 J.K., 0000-0001-6871-5318; A.K., 0000-0002-8154-0257

Here, we set out to analyze a possible role of Notch signaling in visceral SMC differentiation in the murine ureter. We show that the pathway is essential for the timely activation of expression of *Myocd* and of a group of late SMC structural genes, and, hence, for achieving and maintaining proper peristaltic activity in this organ.

RESULTS

Notch signaling components are expressed in ureter development

To determine the abundance of Notch signaling components in ureter development, we analyzed expression of genes encoding Notch ligands and receptors by RNA *in situ* hybridization on transverse sections of the proximal ureter region of E12.5 to E18.5 wild-type embryos (Fig. S1). *Jag1* was homogeneously expressed in the UE and the UM, with lower levels at E16.5 and E18.5. *Jag2* was robustly expressed in the UE at E14.5. At E16.5 and E18.5, expression in this tissue was predominantly found in the basal cell layer. Expression was also found in endothelial cells of vessels in the outer UM from E12.5 to E18.5. *Dll1* and *Dll3* expression was not detected in ureter development. *Dll4* expression was found in endothelial cells of larger vessels at all stages (Fig. S1A). *Notch1* was weakly expressed in the UE from E12.5 to E16.5, and in some basal cells at E18.5. Expression also occurred in endothelia in the outer UM from E12.5 to E18.5. *Notch2* and *Notch3* were strongly expressed in the UM at E12.5 and E14.5, and more weakly at E16.5 and E18.5. *Notch3* expression was additionally found in the UE, and more strongly in perivascular cells in the outer UM from E12.5 to E18.5. *Notch4* expression was associated with endothelia in the outer UM throughout ureter development (Fig. S1B). Expression of *Rbpj* encoding the unique intracellular mediator of this signaling pathway (Jarriault et al., 1995) occurred homogeneously at low level at all stages both in the UM and UE (Fig. S1C).

We next used immunohistochemistry to analyze protein expression of those pathway components for which we had detected mRNA expression in the UM and/or the UE. As we did not find a suitable antibody for JAG2, we omitted it from this analysis. JAG1 and NOTCH1 showed low level expression both in the UM and UE at 12.5 and E14.5. Expression in the UE was increased at E18.5. NOTCH1 was additionally found in endothelial linings of vessels. NOTCH2 was detected in the UM and UE at all analyzed stages. NOTCH3 and RBPJ expression was weak in the UM and UE at E12.5 and E14.5. Expression was strongly increased in the UM and decreased in the UE at E16.5 and E18.5. NOTCH3 was also strongly expressed in vessel walls, including that of the dorsal aorta, at all stages (Fig. 1A).

To test for direct interaction of JAG1 with any of the NOTCH receptors, we performed a proximity ligation assay. We found proximity signals for JAG1 with all three NOTCH receptors in the UM and UE at all stages except E16.5. The JAG1-NOTCH3 interaction appeared strongest at all stages but was still markedly lower than that observed in the dorsal aorta (Fig. 1B).

To test for Notch pathway activity, we analyzed expression of direct transcriptional targets of RBPJ, namely *Hes* and *Hey* genes, and *Nrarp* in ureter development. *Hes1* was strongly expressed in the UE at E12.5, E14.5 and E18.5. *Hes2* and *Hes5* expression was found in both the UE and UM at these stages. *Hes6* and *Hes7* were weakly found in the UM at E12.5 (Fig. S2A). Weak expression of *Hey1* was detected in the UM at E14.5, of *Hey2* in the UM at E12.5 and of *Hey1* in the UM at E12.5, E14.5 and E18.5. Higher levels of *Hey1* and *Hey2* expression were found in endothelial cells of larger vessels, and of *Hey1* in the surrounding vascular SMCs (Fig. S2B). *Nrarp* expression was widespread, but increased in the UM at E14.5

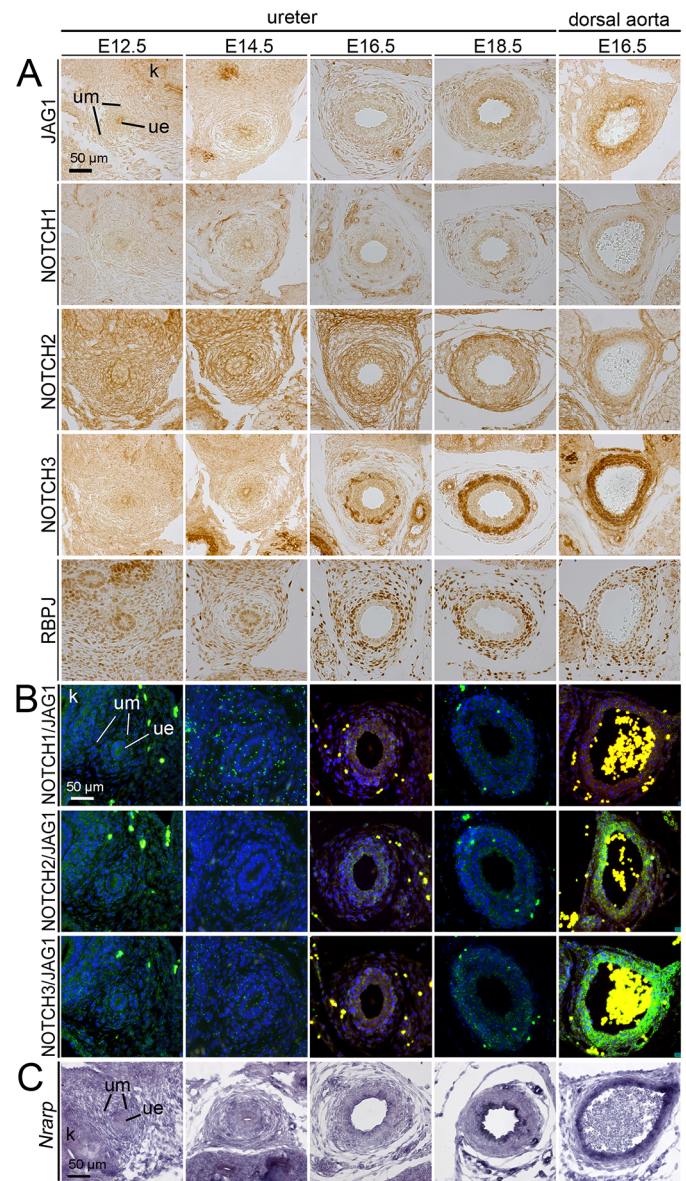


Fig. 1. Notch signaling components are expressed and functionally interact in murine ureter development. (A) Immunohistochemical analysis of expression of the Notch ligand JAG1, the Notch receptors NOTCH1, NOTCH2 and NOTCH3, and the signaling mediator RBPJ. (B) Proximity ligation assay of JAG1 interaction with NOTCH1, NOTCH2 and NOTCH3. (C) *In situ* hybridization analysis of *Nrarp* expression. All assays were performed on transverse sections of the proximal ureter of E12.5, E14.5, E16.5 and E18.5 embryos, and of the dorsal aorta of an E16.5 embryo as a control region for specificity and expression in the vascular system. $n \geq 3$ for all probes and assays. k, kidney; ue, ureteric epithelium; um, ureteric mesenchyme.

and E18.5. Expression in the UE was strong at E16.5 and E18.5, and in vessels at all stages (Fig. 1C). This dataset points to a biphasic wave of Notch signaling activity in the UM, peaking at E14.5 and E18.5. Signaling activity is reduced compared with that in the mesenchymal wall of vessels but may similarly be promoted by JAG1 interaction with NOTCH2 and NOTCH3.

Conditional inactivation of *Rbpj* in the UM leads to changes in SMC differentiation at E18.5

To investigate the role of canonical Notch signaling in the UM, we employed a tissue-specific gene inactivation approach using a

Tbx18^{cre} line generated in our laboratory (Airik et al., 2010) and a floxed allele of *Rbpj* (synonym *Rbpj^{fl}*) (Tanigaki et al., 2002), the unique intracellular mediator of this signaling pathway (Jarriault et al., 1995). *Tbx18^{cre}* mediates recombination in precursors of all differentiated cell types of the UM: fibroblasts of the inner *lamina propria* and the outer *tunica adventitia*, SMCs of the medial *tunica muscularis* (Bohnenpoll et al., 2013) and vascular SMCs but not endothelial cells (Fig. S3). Absence of RBPJ expression in the UM of *Tbx18^{cre/+};Rbpj^{fl/fl}* (*Rbpj-cKO*) embryos confirmed the suitability of our approach (Fig. S4).

We started our phenotypic analysis at the end of embryogenesis, at E18.5, when all differentiated cell types of the ureter are established. At this stage, the urogenital system of *Rbpj-cKO* embryos was morphologically unaffected with the exception of the ureter, which appeared more translucent than in the control (Fig. 2A). The kidney was histologically normal but the *tunica muscularis* of the ureter appeared less condensed (Fig. S5, Fig. 2B). Expression of the SMC proteins ACTA2, TAGLN and NOTCH3 was unchanged in the *tunica muscularis* of the mutant ureter but was reduced in large adventitial vessels (Fig. 2C). Expression of the

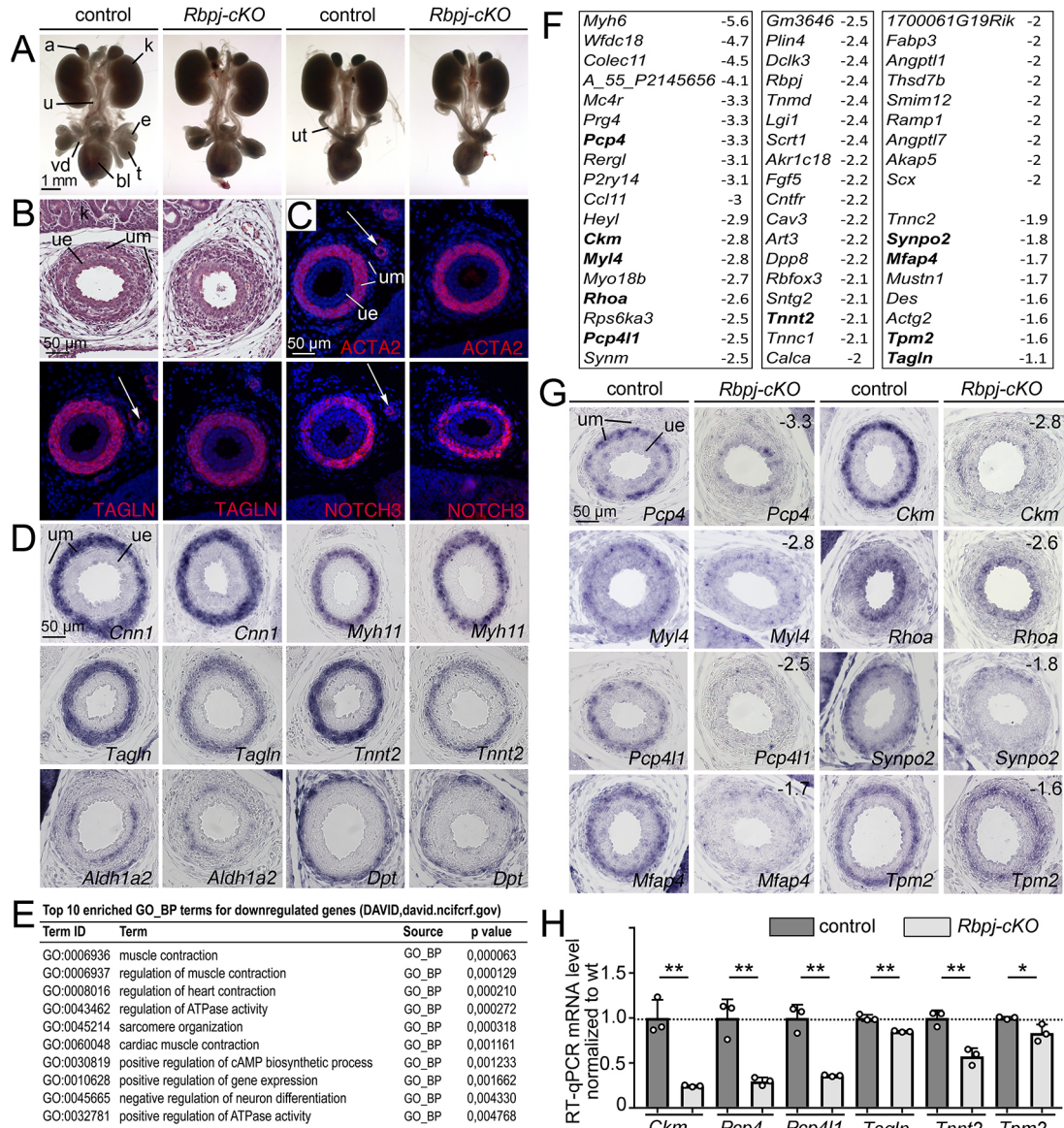


Fig. 2. *Rbpj-cKO* ureters exhibit SMC defects at E18.5. (A) Morphology of whole urogenital systems of male (columns 1 and 2) and female (columns 3 and 4) E18.5 control and *Rbpj-cKO* embryos; $n > 10$ for each sex and genotype. (B-D) Analysis of transverse sections of the proximal ureter region of E18.5 control and *Rbpj-cKO* embryos by Hematoxylin and Eosin staining (B); by immunofluorescence of the SMC marker proteins ACTA2, TAGLN and NOTCH3 [nuclei (blue) are counterstained with DAPI; white arrows indicate vascular SMCs] (C); and by RNA *in situ* hybridization analysis on transverse sections of the proximal ureter for SMC marker genes (*Cnn1*, *Myh11*, *Tagln* and *Tnnt2*), the *lamina propria* marker *Aldh1a2* and the adventitial marker *Dpt* (D). (E) List of top 10 gene ontology (GO) annotations over-represented in the set of genes with reduced expression in E18.5 *Rbpj-cKO* ureters using DAVID web software. (F) List of genes with reduced expression (≤ -1.9) and selected candidates in the microarray analysis of E18.5 *Rbpj-cKO* ureters. In bold are genes with validated expression in the *tunica muscularis* of control ureters. (G) RNA *in situ* hybridization analysis on transverse sections of the proximal ureter at E18.5 for microarray candidate genes. The numbers indicate the fold downregulation. (B-D, G) $n \geq 3$ for all assays and probes. (H) RT-qPCR results for expression of selected SMC structural genes in three independent RNA pools of E18.5 control and *Rbpj-cKO* ureters. Differences were considered significant at $*P < 0.05$ or highly significant at $**P < 0.01$ (two-tailed Student's *t*-test). For values and statistics, see Table S4A. Data are mean \pm s.d. adrenal gland; bl, bladder; e, epididymis; k, kidney; t, testis; u, ureter; ue, ureteric epithelium; um, ureteric mesenchyme; ut, uterus; vd, vas deferens.

SMC structural genes *Cnn1* and *Myh11* appeared unaffected, whereas *Tagln* was weakly reduced and *Tnnt2* was strongly reduced in the ureteric muscle layer. The lamina propria marker *Aldh1a2* and the adventitial marker *Dpt* were unchanged (Fig. 2D). The distribution of endomucin (EMCN) (Morgan et al., 1999) and of KRT5, Δ NP63 and UPK1B (Bohnenpoll et al., 2017a) reflected normal vascular endowment and urothelial differentiation, respectively (Fig. S6A).

To profile transcriptional changes in E18.5 *Rbpj-cKO* ureters in a global and unbiased fashion, we used microarray analysis. Using a threshold of at least a 1.5-fold change and an expression intensity robustly above background (>100), we detected 93 genes with reduced expression and 45 with increased expression in *Rbpj-cKO* ureters (Table S1A,B; deposited in GEO under accession number GSE169662). Functional annotation using the DAVID software tool (Huang da et al., 2009) revealed a highly significant enrichment of gene ontology (GO) terms and clusters related to ‘muscle contraction’ for the pool of downregulated genes, whereas variable terms and clusters with low significance were found for the pool of upregulated genes (Fig. 2E, Tables S2, S3). Manual inspection of the list of downregulated genes detected *Rbpj* (-2.4) and the Notch effector gene *Heyl* (-2.9), confirming the loss of Notch signaling activity. *Tnnt2* expression was strongly reduced (-2.1), *Tagln* (-1.1), *Cnn1* (-1.3) and *Myh11* (-1.3) were weakly reduced, and *Acta2* was unchanged, largely confirming our *in situ* hybridization analysis (Fig. 2F, Table S1A).

We validated expression of a subset of the downregulated genes by *in situ* hybridization analysis. We found strongly reduced expression of *Pcp4*, *Ckm*, *Myl4*, *Pcp411*, *Mfap4*, *Rhoa* and *Synpo2* in the muscle layer of the mutant ureter. *Tpm2* appeared weakly affected; other candidates were not detected by this method (Fig. 2G, Fig. S7). Reverse transcriptase-quantitative PCR (RT-qPCR) confirmed slightly reduced (*Tagln* and *Tpm2*) and strongly reduced (*Ckm*, *Pcp4*, *Pcp411* and *Tnnt2*) expression of SMC genes at this stage (Fig. 2H, Table S4A). We conclude that *Rbpj-cKO* ureters exhibit defects in visceral SMC differentiation shortly before birth.

Loss of *Rbpj* in the UM leads to hydroureter in adolescent mice

To investigate whether expression of SMC genes is merely delayed and normalizes after birth, we analyzed *Rbpj-cKO* ureters at postnatal day (P) 4. At this stage, compartmentalization of the ureter was histologically unaffected but the muscle layer appeared less condensed (Fig. 3A). Immunofluorescence analysis detected normal expression of the SMC proteins ACTA2, TAGLN and NOTCH3 (Fig. 3B), and of the epithelial markers KRT5, Δ NP63 and UPK1B (Fig. S6B). *In situ* hybridization and/or RT-qPCR analysis uncovered that transcripts of SMC genes were differentially affected in their expression: *Cnn1*, *Myh11*, *Tagln* and *Tpm2* appeared unaffected; expression of *Ckm*, *Pcp4*, *Pcp411*, *Myl4* and *Tnnt2* was strongly reduced (Fig. 3C,D; Table S4B). Transcriptional profiling by microarray analysis detected 141 transcripts with reduced expression and 88 with increased expression (>1.5 -fold change, expression intensity >100) in P4 *Rbpj-cKO* ureters (Table S5; deposited in GEO under accession number GSE184597). Functional annotation revealed a significant enrichment of GO terms related to both ‘lipid and glucose metabolism’ and ‘muscle’ for the pool of downregulated genes, whereas GO terms related to ‘extracellular matrix’ were enriched in the pool of upregulated genes (Tables S6 and S7), indicating possible metabolic and structural compensatory mechanisms.

Notably, 25 of the genes with decreased expression at P4 also showed decreased expression at E18.5, yet with fold changes that were reduced compared with that at E18.5 (Fig. 3E). Functional annotations showed an enrichment of terms related to ‘muscle’, ‘Z-disc’, ‘sarcolemma’ and ‘heart muscle’, indicating that common downregulated genes mainly relate to SMC differentiation (Table S8). Expression changes of additional SMC genes fell below the threshold at P4 (Fig. 3E).

To determine whether the SMC defects further decrease with time, we analyzed urogenital systems at P14. At this stage, the mutant ureter was invariably dilated at the proximal level. Some SMC genes seemed unchanged (*Cnn1*, *Myh11* and *Tpm2*), others were strongly reduced (*Ckm*, *Pcp4*, *Pcp411*, *Tagln* and *Tnnt2*) in their expression (Fig. 3F). Together, this shows that SMC differentiation defects, although decreasing after birth, cannot be functionally compensated for and lead to hydroureter formation in early adolescence.

SMC differentiation is delayed in *Rbpj-cKO* ureters

To define the onset of SMC defects in *Rbpj-cKO* ureters, we performed histological and molecular analyses at stages (E14.5 to E16.5) when the SMC phenotype is progressively established. Histological analysis showed that the UM of the mutant was subdivided into an inner layer with rhomboid-shaped condensed cells and an outer layer with loosely organized fibroblast-like cells at all analyzed stages, as in the control, but the inner layer appeared less condensed at E15.5 and E16.5 (Fig. 4A). In the control, expression of ACTA2, TAGLN, *Cnn1*, *Myh11*, *Tagln* and *Tpm2* commenced at E15.5; that of NOTCH3 and *Tnnt2* began at E16.5 in the inner layer of the UM. In *Rbpj-cKO* ureters, expression of *Cnn1*, *Myh11* and *Tpm2* occurred normally from E15.5 onwards. ACTA2, TAGLN and *Tagln* expression was reduced at E15.5 and at E16.5; NOTCH3 and *Tnnt2* expression was not observed in the mutants at E16.5 (Fig. 4B, C). *Ckm*, *Myl4*, *Pcp4* and *Pcp411* mRNA expression was neither detected in the control nor in the mutant ureter in the analyzed time window (Fig. S8). We conclude that loss of *Rbpj* in the UM affects the staggered activation of SMC genes in the fetal ureter.

Rbpj-cKO ureters display delayed and altered peristaltic contractions

We next investigated whether the observed changes in visceral SMC differentiation are accompanied by functional deficits in ureter contractility in explant cultures. Explants of E14.5 *Rbpj-cKO* ureters exhibited a 1.5-day delay in onset of peristaltic activity (Fig. 5A,B, Table S9A). The contraction frequency was significantly decreased until day 6 and reached control levels only at day 7 and 8 of the culture (Fig. 5C, Table S9B). The contraction intensity was strongly reduced at all analyzed levels throughout the entire contraction wave at day 4 of the culture. At the endpoint, day 8, the initial contraction velocity in the proximal and the medial part was normal but the contraction intensities remained lower throughout the contraction wave (Fig. 5D, Table S9C).

Mutant ureters explanted at E18.5 exhibited a significantly reduced contraction frequency at day 1 and 2 of culture but reached the level of the control from day 3 onwards (Fig. 5E,F, Table S10A). At day 1, the contraction occurred less rapidly and reached lower intensities; the relaxation wave was, however, unaffected. At day 3, the mutant ureters reached the contraction intensity of the control, albeit with a slight but significant delay. At day 6, the mutant ureters reached higher contraction intensities and maintained them for longer. This was most prominent at the medial position (Fig. 5G, Table S10B).

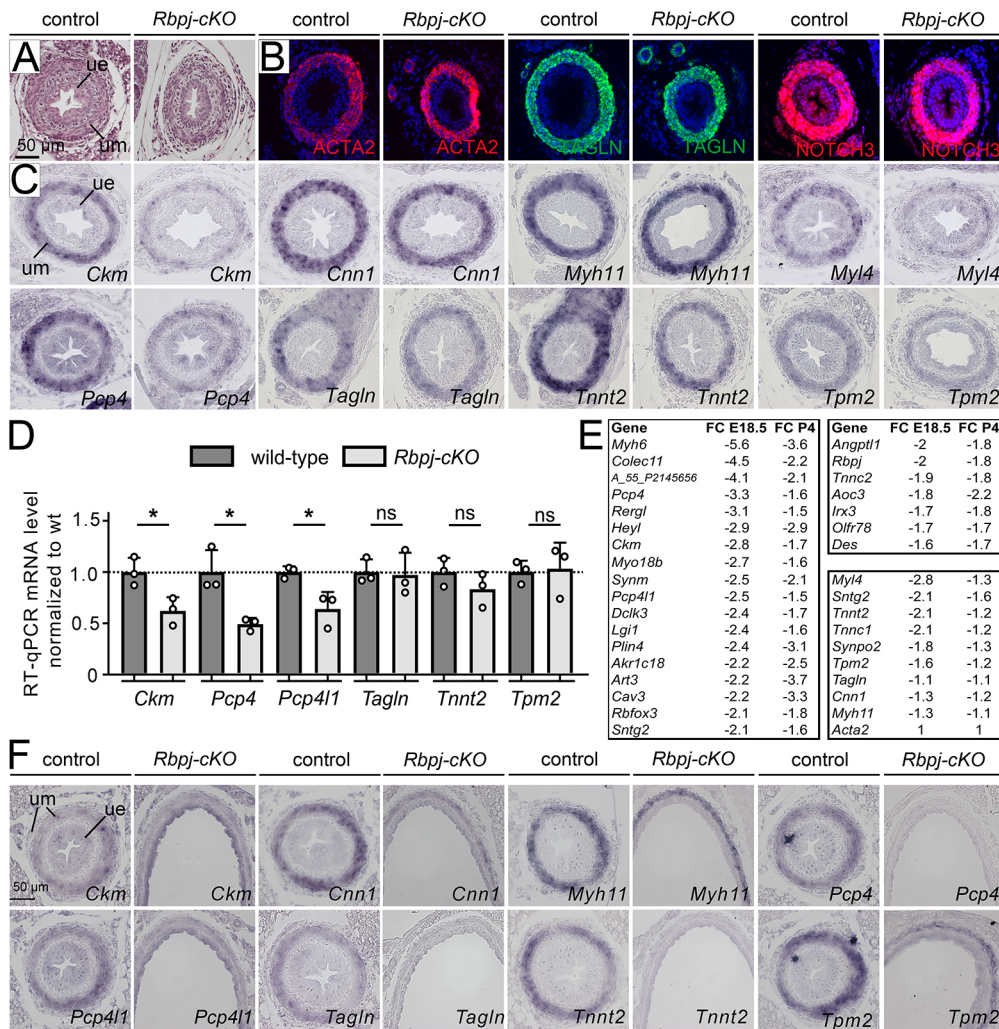


Fig. 3. SMC differentiation is affected in *Rbpj-cKO* ureters at postnatal stages. (A-C) Hematoxylin and Eosin staining (A), immunofluorescence of SMC proteins (B) and RNA *in situ* hybridization analysis of expression of SMC marker genes (C) on transverse sections of the proximal ureter region of control and *Rbpj-cKO* embryos at P4. $n \geq 3$ for all probes. (D) RT-qPCR results for expression of selected SMC structural genes in three independent RNA pools of control and *Rbpj-cKO* ureters at P4. Differences were considered non-significant (ns) at $P > 0.05$, significant at $*P < 0.05$ (two-tailed Student's *t*-test). For values and statistics, see Table S4B. Data are means \pm s.d. (E) List of genes with reduced expression in microarrays of both E18.5 and P4 *Rbpj-cKO* ureters (left box and upper right box), and a short list of additional SMC genes (lower right box). Shown are the average fold changes (FC) at the two stages. (F) *In situ* hybridization analysis of SMC genes on proximal sections of control and *Rbpj-cKO* ureters at P14. The mutant ureter is dilated. $n \geq 3$ for all probes. ue, ureteric epithelium; um, ureteric mesenchyme.

Hence, loss of *Rbpj* affects onset and progression of the peristaltic activity of the fetal and perinatal ureter. At perinatal stages, ureter contractility appears weakly affected, indicating that, in the absence of hydrostatic pressure, deficits in the SMC program can be functionally compensated for.

Loss of *Rbpj* affects onset of *Myocd* expression in the UM

To identify molecular changes that may cause delayed and reduced SMC differentiation in *Rbpj-cKO* ureters in an unbiased fashion, we performed microarray-based gene expression profiling of E14.5 ureters. Using an intensity threshold of 100 and fold changes of at least 1.5 in the two individual arrays, we detected 30 genes with increased and 16 with decreased expression in mutant ureters (Fig. 6A; Table S11A,B; deposited in GEO under accession number GSE169661).

Functional annotation revealed an enrichment of GO terms related to the differentiation of secretory cells, dopaminergic neurons and/or chromaffin cells in the pool of upregulated genes, but *in situ* hybridization did not detect expression of any of the selected candidates in control and mutant ureters (Table S12A, Fig. S9). In the pool of downregulated genes, GO terms related to protein binding and negative regulation of WNT signaling (*Mdfr*, *Shisa2* and *Wif1*) were found (Table S12B). Manual inspection of the list identified *Rbpj* (-1.9), confirming the functionality of our genetic approach, and *Myocd* (-2.0), the key

regulator of SMC differentiation (Fig. 6A). *In situ* hybridization detected reduced expression of *Mdfr*, *Car3*, *Shisa2* and *Myocd* in the UM of mutant embryos (Fig. 6B). Other candidates showed unspecific or no expression in control and mutant ureters (Fig. S10).

In agreement with our microarray data, we did not detect expression changes for genes encoding cellular signals, signaling targets and transcription factors that have previously been implicated in *Myocd* activation and SMC differentiation in the ureter by *in situ* hybridization analysis (Fig. S11A,B). These findings validate that reduced expression of the WNT antagonist *Shisa2* does not translate into changes in WNT signaling, and that known regulators of *Myocd* expression are unchanged in E14.5 *Rbpj-cKO* ureters.

To determine whether *Myocd* expression is delayed in *Rbpj-cKO* ureters, we analyzed its expression at subsequent stages. *In situ* hybridization detected normal expression at E15.5, E16.5, E18.5 and P4 (Fig. 6C). RT-qPCR analysis confirmed strongly reduced expression of *Myocd* at E14.5, whereas expression of *Foxf1*, an activator of *Myocd* expression, was unchanged (Fig. 6D, Table S4C). Expression of *Myocd* was unchanged in this assay at E18.5 and P4, supporting the *in situ* hybridization results (Fig. 6E, Table S4D). We conclude that *Rbpj*-dependent Notch signaling is required for precise activation of *Myocd* at E14.5 but not for its further maintenance at fetal and postnatal stages.

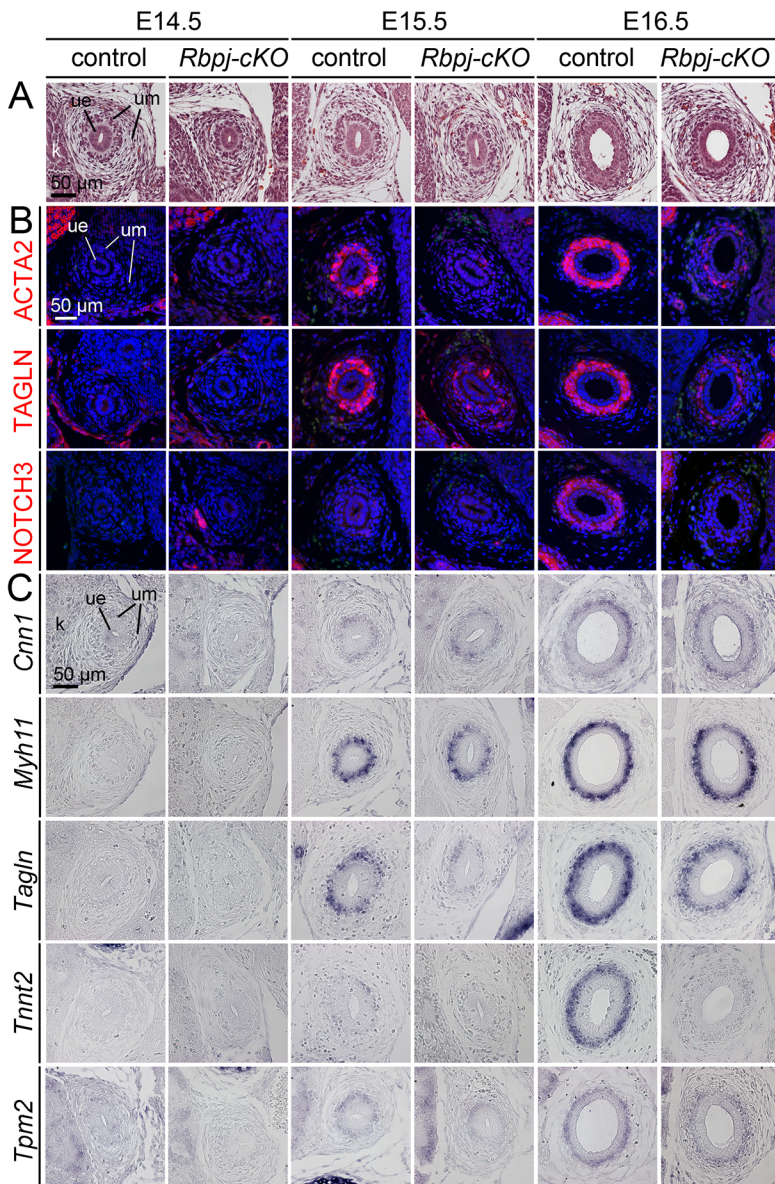


Fig. 4. Onset of SMC differentiation is affected in *Rbpj-cKO* ureters. (A-C) Hematoxylin and Eosin staining (A), immunofluorescent analysis of SMC proteins (B) and RNA *in situ* hybridization analysis of expression of SMC marker genes (C) on transverse sections of the proximal ureter region of control and *Rbpj-cKO* embryos at E14.5, E15.5 and E16.5. $n \geq 3$ for all probes and stages. k, kidney; ue, ureteric epithelium; um, ureteric mesenchyme.

Notch signaling is required for onset and maintenance of SMC differentiation in the ureter

To exclude the possibility that RBPJ acts independently of Notch receptors in the context of the UM, and to distinguish early from late requirements of this pathway, we performed time-controlled pharmacological Notch pathway interference experiments with the γ -secretase inhibitor DAPT (Cheng et al., 2003) in ureter explant cultures. Administration of 1 μ M and 2.5 μ M DAPT (Cheng et al., 2003) to E12.5 ureter explants led to a dose-dependent delay in the onset of the peristaltic activity and a reduction of contraction frequency, similar to the situation observed in explants of E14.5 *Rbpj-cKO* ureters (Fig. 7A,B, Table S13).

We next explanted wild-type ureters at E18.5 and treated them with 1 μ M of DAPT. These ureters showed a normal peristaltic onset but a reduced contraction frequency until day 3 of culture, again similar to *Rbpj-cKO* ureters (Fig. 7C, Table S14). After 18 h in culture, expression of *Ckm* and *Tnnt2* was significantly reduced; *Pcp411* and *Tpm2* showed a strong trend towards reduction. Expression of *Myocd*, *Pcp4* and *Tagln* appeared unaffected (Fig. 7D, Table S4E).

Wild-type ureter explanted at P4 and treated with 1 μ M of DAPT exhibited normal peristaltic contractions in a 6-day culture period (Fig. 7E, Table S15). After 18 h in culture, expression of *Ckm*, *Pcp4*, *Tagln* and *Tnnt2* was reduced, while *Myocd*, *Pcp411* and *Tpm2* appeared unchanged (Fig. 7F, Table S4F).

Hence, loss of Notch signaling affects onset and progression of the peristaltic activity of the fetal and perinatal ureter. Reduced expression of SMC genes at perinatal and postnatal stages is independent of *Myocd* expression.

Notch signaling is not sufficient to induce SMC development

We finally asked whether Notch signaling is sufficient to induce SMC relevant genes in ureter development. For this, we combined our *Tbx18^{cre}* driver line with a *Rosa26* knock-in allele (*Rosa26^{NICD}*) (Murtaugh et al., 2003), allowing conditional expression of the Notch1 intracellular domain (NICD) in the undifferentiated UM. As *Tbx18^{cre/+};Rosa26^{NICD/+}* embryos died around E13.5 (Grieskamp et al., 2011), we used E12.5 ureters for section *in situ* hybridization analysis. We did not find ectopic and/or precocious expression of the SMC regulators *Foxf1* and *Myocd*, of SMC

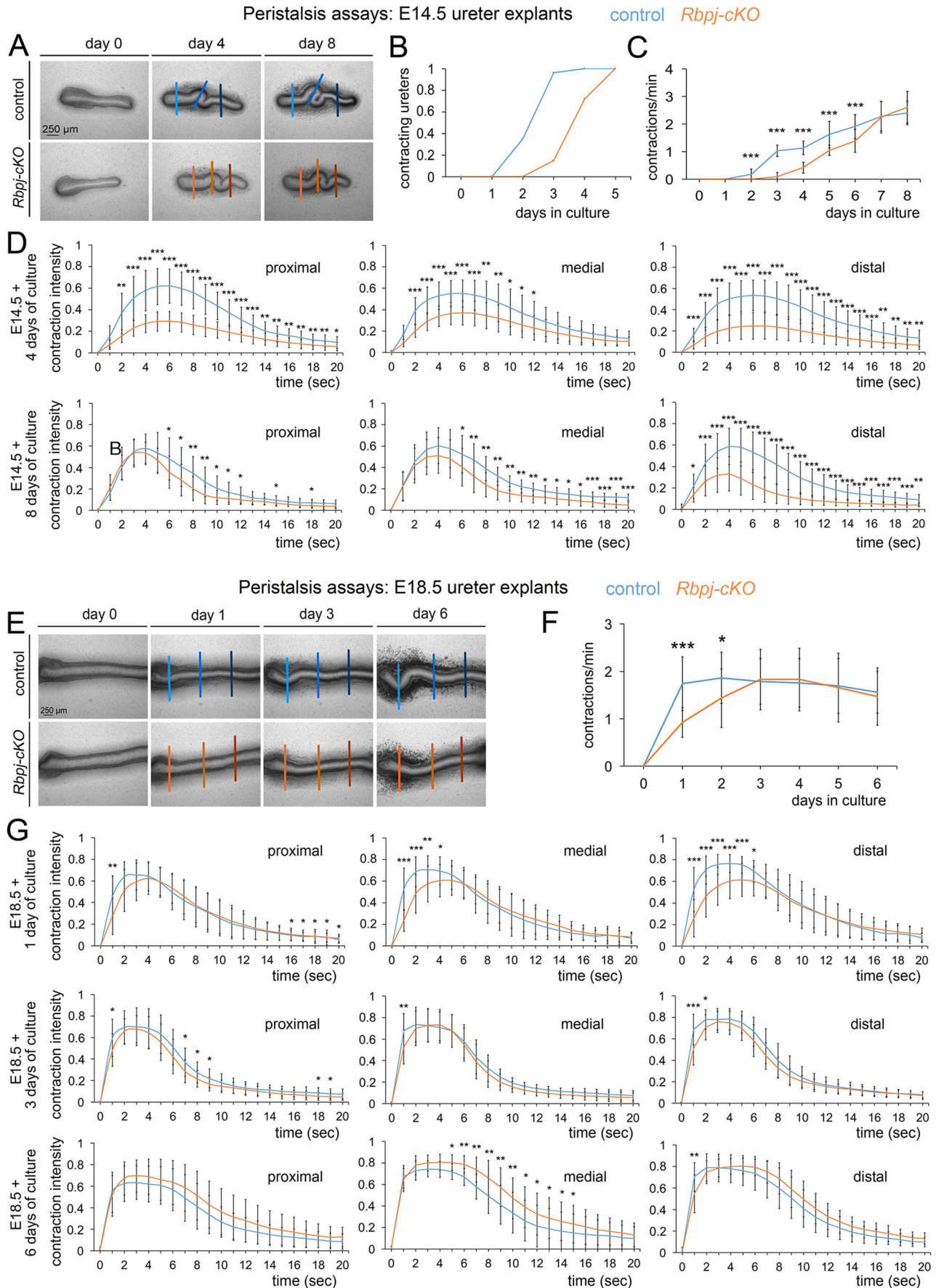


Fig. 5. See next page for legend.

Fig. 5. Peristaltic activity of *Rbpj*-cKO ureters is affected at fetal and perinatal stages. (A-D) Analysis of peristaltic contractions of E14.5 ureter explants in culture; control, $n=23$; *Rbpj*-cKO, $n=16$. (A) Morphological analysis by bright-field microscopy. Vertical lines indicate the positions along the ureter at which contraction intensities were measured during one contraction wave at day 4 and day 8 of culture. Positions relate to 25% (proximal), 50% (medial) and 75% (distal) of ureter length. (B) Analysis of contraction onset in an 8-day culture period. For statistical values, see Table S9A. (C) Analysis of the contraction frequency in E14.5 ureter explants cultured for 8 days. For statistical values, see Table S9B. (D) Analysis of the contraction intensity at proximal, medial and distal levels of E14.5 ureter explants at day 4 and day 8 of culture. For statistical values, see Table S9C. Differences were considered significant at $*P<0.05$, highly significant at $**P\leq 0.01$ and extremely significant at $***P\leq 0.001$ (two-tailed Student's *t*-test) (B-D). Data are mean \pm s.d. (E-G) Analysis of peristaltic contractions of E18.5 ureter explants in culture; control, $n=26$; *Rbpj*-cKO, $n=16$. (E) Morphological analysis by bright-field microscopy. Vertical lines indicate the positions along the ureter at which contraction intensities were measured during one contraction wave. Positions relate to 25% (proximal), 50% (medial) and 75% (distal) of ureter length. (F) Analysis of contraction onset and frequency in a 6-day culture period. For values and statistics, see Table S10A. (G) Analysis of the contraction intensity at proximal, medial and distal levels of ureters explanted at E18.5 and cultured for 1, 3 and 6 days. For statistical values, see Table S10B. Differences were considered significant at $*P\leq 0.05$, highly significant at $**P\leq 0.01$ and extremely significant at $***P\leq 0.001$ (two-tailed Student's *t*-test) (F,G). Data are mean \pm s.d.

structural genes, or of *Car3* and *Shisa2*, indicating that Notch signaling is required but not sufficient to activate SMC regulatory and structural genes in the developing ureter (Fig. S12). To analyze the effect of NIICD overexpression in the UM at late fetal stages, we combined a tamoxifen-inducible variant of *Tbx18* (*Tbx18^{CreERT2}*) with the *Rosa26^{NIICD}* allele, explanted mutant ureters at E13.5 and cultured them for 4 days in the presence of tamoxifen. Enhanced expression of *Hey1* showed the suitability of the approach. Similar to induced *Hey1* expression, SMC markers appeared more patchy, but levels were decreased rather than increased in some cases (Fig. S13) indicating that a (low) level of Notch signaling in the UM is important for ureteric SMC integrity.

DISCUSSION

Notch signaling is a novel regulator of SMC differentiation in the ureter

Previous genetic work provided compelling evidence that Notch signaling is a crucial regulator of vascular SMC differentiation (for reviews, see Baeten and Lilly, 2017; Fouillade et al., 2012). This applies both to neural crest cells, from which SMCs of the great vessels, including the aorta, are derived (Feng et al., 2010; High et al., 2007; Manderfield et al., 2012), as well as to mesothelial cells and other progenitors of arterial SMCs in different organ systems (Etchevers et al., 2001; Grieskamp et al., 2011; Volz et al., 2015). In either case, loss of Notch signaling (components) was associated with severely reduced expression of SMC structural genes, including early differentiation markers ACTA2 and TAGLN, and with subsequent vessel dilatation.

To unravel the function of Notch signaling in the development of the UM, we used a combination of genetic and pharmacological pathway inhibition experiments. Loss of the Notch signaling mediator *Rbpj* affected neither ureter shape and length nor the subdivision of its mesenchymal wall at fetal and postnatal stages, excluding a role of the pathway in survival, proliferation and patterning of the UM. At newborn stages, a set of important SMC proteins/genes (*ACTA2*, *TAGLN*, *Myh11* and *Cnn1*) was correctly expressed in the medial region of the UM, indicating that visceral SMC specification and early differentiation of SMCs has occurred

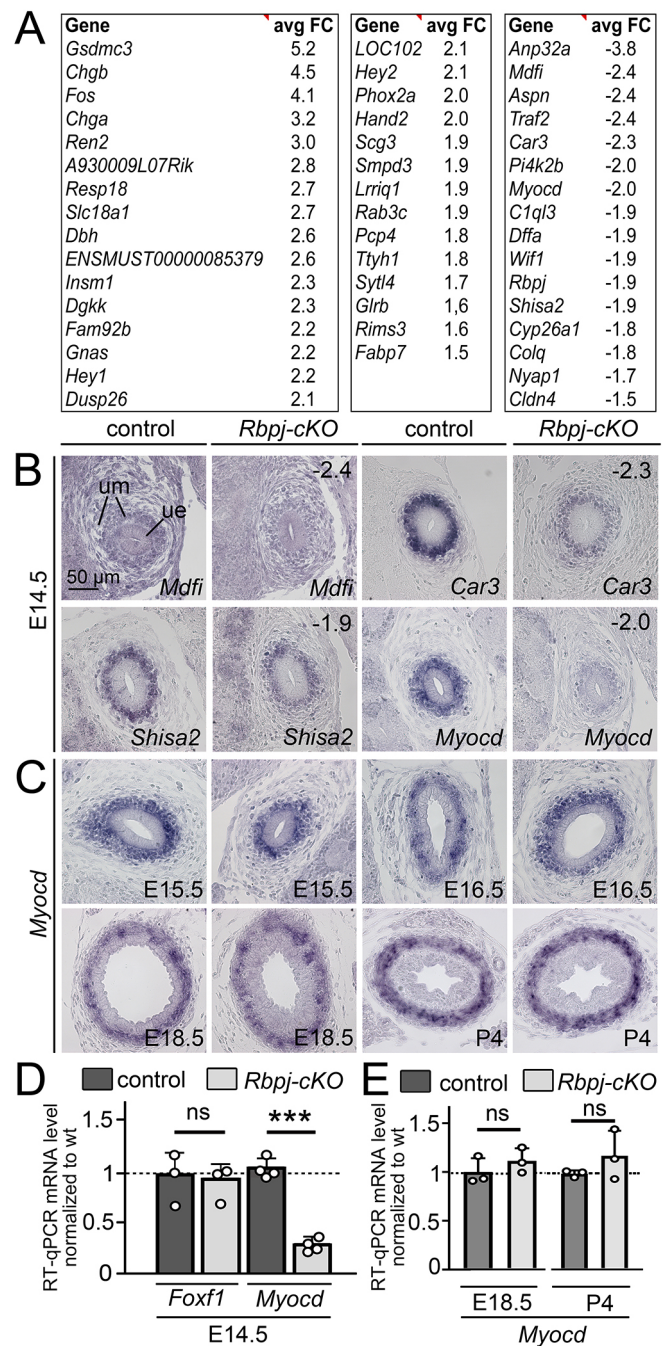


Fig. 6. Onset of *Myocd* expression is affected in *Rbpj*-cKO ureters. (A) List of genes with increased [average fold change (avgFC) ≥ 1.5] and reduced expression (avgFC ≤ -1.5) in the microarray analysis of E14.5 *Rbpj*-cKO ureters. (B,C) RNA *in situ* hybridization analysis on transverse sections of the proximal ureter of control and *Rbpj*-cKO embryos for expression of microarray candidate genes at E14.5 (B) and for *Myocd* expression at E15.5, E16.5, E18.5 and P4 (C). $n\geq 3$ for all probes. (D,E) RT-qPCR results for expression of *Foxf1* and *Myocd* in RNAs pools of control and *Rbpj*-cKO ureters at E14.5 (D), and of *Myocd* expression in E18.5 and P4 ureters (E). Differences were considered non-significant (ns) at $P>0.05$, and extremely significant at $***P\leq 0.001$ (two-tailed Student's *t*-test). For values and statistics, see Table S4C,D. Data are mean \pm s.d. ue, ureteric epithelium; um, ureteric mesenchyme.

normally. However, we observed a delayed expression onset of *Myocd* and of 'early' SMC genes around E14.5 and E16.5, as well as a delayed onset and reduced expression of a set of 'late' SMC

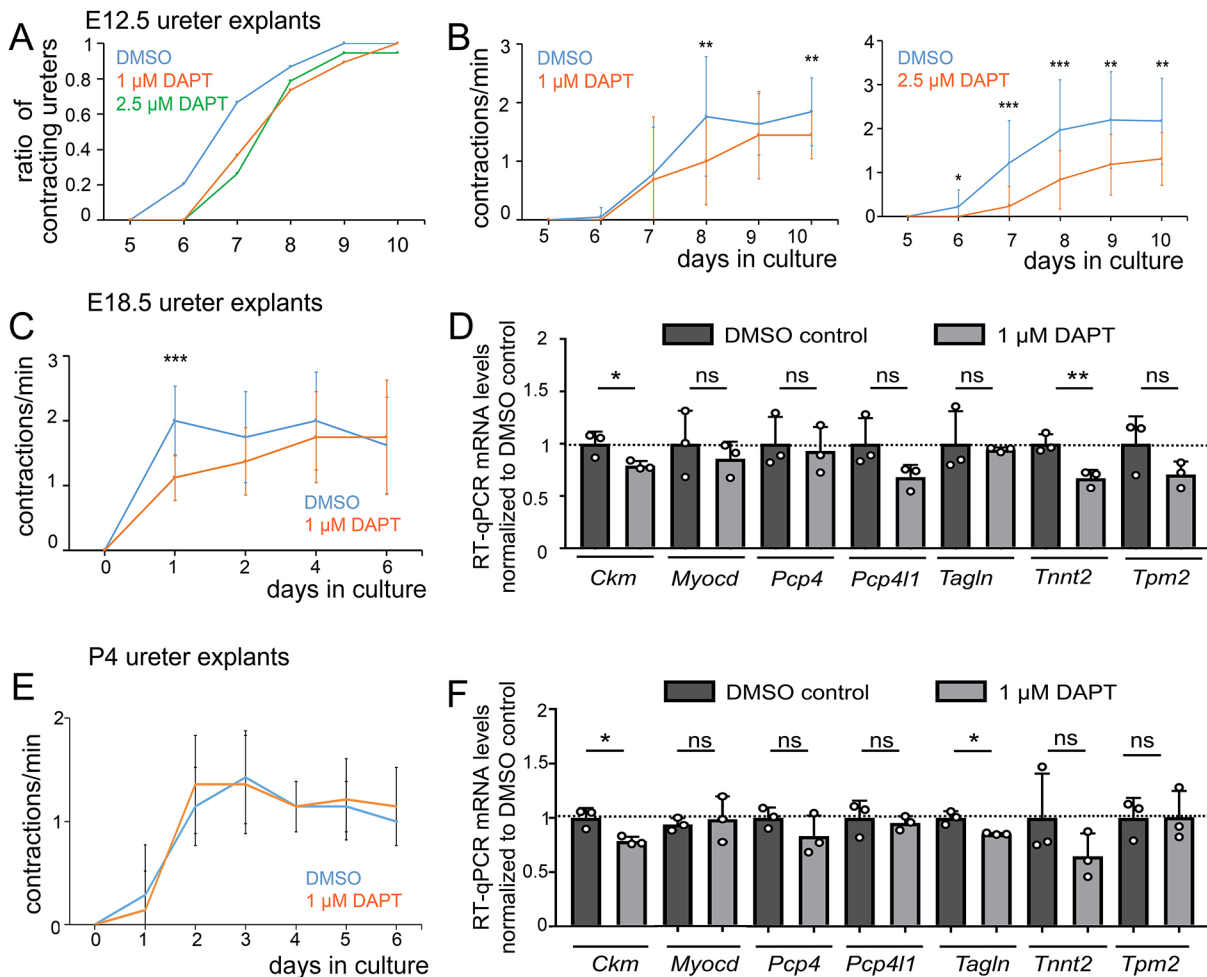


Fig. 7. Pharmacological inhibition of Notch signaling affects SMC differentiation and peristaltic activity of the fetal and perinatal ureter. (A,B) Analysis of onset (A) and frequency (B) of peristaltic contractions in explant cultures of E12.5 wild-type ureters treated with DMSO (control, $n=19$) or with 1 μM of the Notch signaling inhibitor DAPT ($n=19$), and with DMSO (control, $n=20$) or 2.5 μM DAPT ($n=19$). For values and statistics, see Table S13. (C) Analysis of frequency of peristaltic contractions in explant cultures of E18.5 wild-type ureters treated with DMSO (control, $n=8$) or with 1 μM DAPT ($n=8$). For values and statistics, see Table S14. (D) RT-qPCR results of expression of selected SMC genes in three independent RNA pools of wild-type ureters explanted at E18.5 and cultured for 18 h in FCS-free (ITS) medium supplemented with DMSO (control) or with 1 μM DAPT. For values and statistics, see Table S4E. (E) Analysis of frequency of peristaltic contractions in explant cultures of P4 wild-type ureters treated with DMSO (control, $n=7$) or with 1 μM DAPT ($n=7$). For values and statistics, see Table S15. (F) RT-qPCR results of expression of selected SMC genes in three independent RNA pools of P4 wild-type ureters cultured for 18 h in FCS-free (ITS) medium supplemented with DMSO (control) or with 1 μM DAPT. For values and statistics, see Table S4F. Differences were considered significant at $*P \leq 0.05$, highly significant at $**P \leq 0.01$ and extremely significant at $***P \leq 0.001$ (two-tailed Student's *t*-test). Data are mean \pm s.d.

genes in *Rbpj-cKO* ureters at fetal and postnatal stages. At the physiological level, these changes translated into a delayed onset of peristaltic activity, reduced contraction frequency and intensity at fetal stages. Time-controlled pharmacological Notch pathway inhibition experiments largely recapitulated these phenotypic changes, confirming a role for Notch signaling and RBPJ in timing, modifying and/or fine-tuning visceral SMC differentiation in the ureter.

Rbpj deficiency or Notch pathway inhibition did not affect peristaltic activity of P4 ureters *ex vivo*, suggesting that the SMC defects at this stage are minor. However, and to our surprise, *Rbpj-cKO* ureters exhibited ureter dilatation (hydroureter) at P14, indicating that the mutant SMC layer has reduced capacity to withstand the hydrostatic pressure of the urine with time. The phenotypic burden of *Rbpj-cKO* mice prevented analysis at later stages in adults. However, it is likely that, under the permanent pressure exerted by the urine, even a weak reduction of SMC structural proteins will cause further deficits of SMC contractility

and rigidity that will translate in progressive ureter dilatation, hydronephrosis and end-stage renal disease. Mutations that affect expression of Notch components may therefore underlie human congenital anomalies of the kidney and ureteric tract (CAKUT), a group of diseases for which the genetic cause has only partly been resolved (Kohl et al., 2021).

Although not analyzed in any detail, we noted reduced ACTA2 and TAGLN expression in cells surrounding endothelial linings in the adventitial layer of *Rbpj-cKO* ureters, indicating that Notch signaling is essential for vascular SMC differentiation in the ureter as in many, if not all, other organs.

Notch signaling acts in a biphasic manner within the ureteric mesenchyme

Work in the vascular system characterized JAG1, NOTCH2 and NOTCH3 as the major Notch components involved in SMC differentiation (for a review, see Baeten and Lilly, 2017). Endothelial JAG1 serves as the initial cue to activate Notch

signaling in surrounding perivascular cells (High et al., 2008). This leads to increased expression of NOTCH3, as well as JAG1, in these cells, which in turn promotes, by homotypic interaction, their differentiation into SMCs (Hoglund and Majesky, 2012; Liu et al., 2009). Whereas NOTCH3 is expressed in all mural cells, NOTCH2 is mainly found in large vessels, such as the cardiac outflow tract (High et al., 2007; Joutel et al., 2000). Accordingly, *Notch2* and *Notch3* are redundantly required for vascular SMC differentiation in larger vessels, whereas in pericytes and small vessels NOTCH3 is the dominant player (Liu et al., 2010; Volz et al., 2015; Wang et al., 2012). Our expression analysis confirmed the relevance of this JAG1-NOTCH2/NOTCH3 network in vascular SMC development in the dorsal aorta, which we used as ‘control’ tissue. JAG1 was found in the endothelium and surrounding perivascular cells, where co-expression occurred with NOTCH2 and NOTCH3. Strong JAG1-NOTCH2 and particularly JAG1-NOTCH3 interaction in these perivascular cells was validated by the proximity ligation assay.

A similar JAG1-NOTCH2/NOTCH3 module may operate in the UM during development. Our immunohistochemical analysis revealed low level expression of JAG1 and high level expression of NOTCH2 in the UM at all developmental stages. NOTCH3 was strongly upregulated at E16.5 in the UM, reaching levels of expression similar to that seen in the perivascular cells of the dorsal aorta. RBPJ also showed an upregulation in the UM, suggesting that translation of both mRNAs is similarly controlled. Our proximity ligation assay uncovered interaction of JAG1 with NOTCH2 and NOTCH3 from E12.5 to E14.5, and at E18.5, and increased expression of the direct NOTCH target genes *Hey1* and *Nrarp* in the UM at these stages. Although the overall activation of Notch signaling in the UM is clearly much weaker compared with that in perivascular cells of the dorsal aorta, our findings point to a biphasic activation of NOTCH2 and/or NOTCH3 by JAG1 in the UM: first, from E12.5 and E14.5, and then concomitant with the upregulation of NOTCH3 after E16.5. It is noteworthy that, unlike JAG1 and NOTCH2, expression of NOTCH3 is largely cytosolic, raising the possibility that JAG1-NOTCH3 interaction occurs cell-autonomously with the UM. This would be reminiscent of the situation found in pulmonary artery vascular SMCs in the developing lung. There, NOTCH3 is expressed and activated in late fetal to early postnatal life, dependent on SMC-derived JAG1 (Ghosh et al., 2011). Although the presence of a JAG1-NOTCH2/NOTCH3 signaling module in the UM seems highly plausible, we cannot exclude the possibility that epithelial Notch ligands (JAG1 or the strongly expressed JAG2) contribute to activation of Notch receptors in the UM. We deem it unlikely as the presence of an intervening basement membrane and, later, also that of the *lamina propria* layer should prevent the direct contact between the ligand- and receptor-bearing cells required for Notch pathway activation. Conditional gene targeting experiments for individual Notch components may provide conclusive data in the future.

Notch signaling acts in a bimodal manner in ureter development

Our molecular analysis found that a group of ‘early’ SMC structural genes, including ACTA2 and TAGLN are activated with a delay of 1–2 days in *Rbpj-cKO* ureters but reached normal levels of expression at E18.5. Compatible with this expression pattern, we observed a delayed activation of the regulator of the SMC differentiation, *Myocd*, at E15.5 in *Rbpj-cKO* ureters. Importantly, we did not detect changes in the activity of signaling pathways (SHH, BMP4, WNT and RA) and transcription factors (*Foxf1*,

Tshz3 and *Sox9*) that have been implicated in the regulation of *Myocd* at E14.5 (Airik et al., 2010; Bohnenpoll et al., 2017b,c; Caubit et al., 2008; Mamo et al., 2017; Trowe et al., 2012). Hence, *Myocd* may be a direct target of RBPJ or of HES/HEY bHLH proteins that mediate the activity of this pathway in many contexts (Bray and Bernard, 2010; Fischer et al., 2004). Irrespective of the precise mode of action, we posit that Notch signaling provides an important input for precise temporal activation of *Myocd* transcription in the fetal ureter.

Our expression analyses uncovered that a group of SMC structural genes that are normally activated between E17.5 and E18.5 in the UM (including *Ckm*, *Pcp4*, *Pcp4l1* and *Tnnt2*) were not present at E18.5 and showed reduced expression at P4 in *Rbpj-cKO* ureters. Pharmacological Notch signaling inhibition of E18.5 ureters resulted in similar changes. Given unchanged *Myocd* expression in mutant ureters from E15.5 onwards, we suggest that MYOCD/SRF is not sufficient to activate expression of these ‘late’ SMC genes but that Notch signaling provides a crucial second input for their timely activation. Importantly, misexpression of NICD neither prematurely activated nor enhanced expression of any of the SMC genes tested. In fact, enforced Notch signaling at late fetal stages led to a decreased and patchy SMC gene expression. This confirms that Notch is a modulator and not a driver of the visceral SMC program, and that the level of signaling at late fetal stages is tightly controlled to assure integrity of the *tunica muscularis*.

‘Late’ SMC genes affected in *Rbpj-cKO* ureters have been implicated in constriction (*Tnnt2*), relaxation (*Pcp4*) and energy conservation (*Ckm*) of cardiomyocytes, and in cardiomyopathies when deficient (Kim et al., 2014; Rentschler et al., 2012; Walker et al., 2021; Wei and Jin, 2016). Therefore, reduced expression of these genes/proteins may affect constriction and/or relaxation of ureteric SMCs, and contribute to hydronephrosis formation in *Rbpj-cKO* mice.

In the vascular system, Notch signaling regulates and synergizes with PDGFRB and TGF β signaling in activation of early SMC genes (for reviews, see Baeten and Lilly, 2017; Fouillade et al., 2012). We did not find changes in expression of components or targets of these pathways in our transcriptional profiling experiments, suggesting that the molecular circuits regulated by Notch signaling in the control of visceral SMC differentiation are different from those in the vascular context.

In summary, we suggest that JAG1-activated NOTCH2 and/or NOTCH3 signaling regulates visceral SMC differentiation in the UM in a bimodal and biphasic manner. First, the module enhances *Myocd* expression to a critical level at E14.5; second, it enhances from around E17.5 the expression of a set of ‘late’ SMC genes that are crucial for long-term maintenance of ureter peristaltic activity (Fig. 8).

MATERIALS AND METHODS

Mouse strains and husbandry

All alleles used in this study were maintained on an NMRI outbred background: *Rbpj^{fl/fl}* (synonym *Rbpj^{fl}*) (Tanigaki et al., 2002), *Gt(ROSA)26Sor^{tm1(Notch1)Dam}* (synonym *Rosa26^{NICD}*) (Murtaugh et al., 2003), *Tbx18^{tm4(cre)Akis}* (synonym *Tbx18^{cre}*) (Trowe et al., 2010), *Tbx18^{tm3.1(cre/ERT2)Sev}* (synonym *Tbx18^{creERT2}*) (Guimaraes-Cambo et al., 2017) and *Gt(ROSA)26Sor^{tm4(ACTB-tdTomato,-EGFP)Lo}* (synonym *Rosa26^{nTmG}*) (Muzumdar et al., 2007). Embryos for ureter explant cultures and for expression analysis of genes encoding Notch components were obtained from matings of NMRI wild-type mice. *Tbx18^{cre/+};Rbpj^{fl/+}* males were mated with *Rbpj^{fl/fl}* females, and *Tbx18^{cre/+}* or *Tbx18^{creERT2/+}* males were mated with *Rosa26^{NICD/NICD}* females to obtain embryos for phenotypic characterization. Littermates without the *cre/creERT2* allele

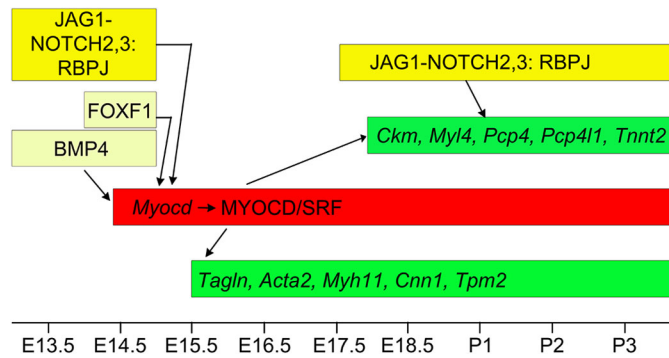


Fig. 8. RBPJ-dependent Notch signaling acts in a biphasic and bimodal fashion in ureter development. Scheme of the temporal activity and function of RBPJ-dependent Notch signaling in the mesenchymal compartment of the developing ureter. JAG1-NOTCH2/NOTCH3-dependent RBPJ activity activates, together with FOXF1 and BMP4 signaling, *Myocd* expression around E14.5. MYOCD in complex with SRF activates expression of early SMC genes (*Tagln*, *Acta2*, *Myh11*, *Cnn1* and *Tpm2*) from E15.5 onwards, and of late SMC genes (*Ckm*, *Myl4*, *Pcp4*, *Pcp4l1* and *Tnnt2*) from around E17.5. JAG1-NOTCH2/NOTCH3-dependent RBPJ activity is also required for timely expression of the late cluster. Length of boxes relates to onset and duration of activity in fetal and early postnatal ureter development, as indicated by the stages at the bottom.

were used as controls. Pregnancies were timed as embryonic day (E) 0.5 by the presence of vaginal plugs the morning after mating. Embryos and urogenital systems were dissected in PBS. Specimens were fixed in 4% PFA/PBS, transferred to methanol and stored at -20°C prior to further processing. PCR genotyping was performed on genomic DNA prepared from liver biopsies or yolk sacs.

Mice were housed in rooms with controlled light and temperature at the central animal laboratory of the Medizinische Hochschule Hannover. The experiments were in accordance with the German Animal Welfare Legislation and approved by the local Institutional Animal Care and Research Advisory Committee and permitted by the Lower Saxony State Office for Consumer Protection and Food Safety (AZ 33.12-42502-04-13/1356, AZ42500/1H).

Organ cultures

Ureters were explanted on 0.4 μm polyester membrane Transwell supports (3450, Corning) and cultured in DMEM/F12 supplemented with 1% of concentrated stocks of penicillin/streptomycin, sodium pyruvate, glutamax, non-essential amino acids and IST-G (insulin-transferrin-selenium) (Thermo Fisher Scientific) at the air-liquid interface as previously described (Bohnenpoll et al., 2013). DAPT (GSI-IX) (S2215, Selleckchem) was used at final concentrations of 1 or 2.5 μM . To induce recombination with the *Tbx18^{creERT2}* line, 4-hydroxytamoxifen (#H7904, Sigma-Aldrich) was used at a final concentration of 500 nM. Culture medium was replaced every 48 h. Analysis of frequencies and intensities of ureter contractions in explant cultures was performed by videomicroscopy as recently described (Weiss et al., 2019).

Histological, histochemical and immunofluorescence analysis

Embryos, urogenital systems or explant cultures were embedded in paraffin wax, and 5 μm sections were cut. Hematoxylin and Eosin staining was performed according to standard procedures.

For immunofluorescence and immunohistochemistry, the following primary antibodies and dilutions were used: polyclonal rabbit-anti-JAG1 (1:200; sc-8303, Santa Cruz Biotechnology), monoclonal mouse-anti-JAG1 (1:200; sc-390177, Santa Cruz Biotechnology), monoclonal rabbit-anti-NOTCH1 (1:200; 3608, Cell Signaling Technology), monoclonal rabbit-anti-NOTCH2 (1:200; 5732, Cell Signaling Technology), polyclonal rabbit-anti-NOTCH3 (1:200; ab23426, Abcam), monoclonal rat-anti-RBPJ (1:200; SIM-2ZRBP3, Cosmo BIO USA), polyclonal rabbit-anti-KRT5 (1:250; PRB-160P, Covance), polyclonal rabbit-anti- ΔNP63 (1:250; 619001,

BioLegend), monoclonal mouse-anti-UPK1B (1:250; WH0007348M2, Sigma-Aldrich), polyclonal rabbit-anti-TAGLN (1:200; ab14106, Abcam), monoclonal mouse-anti-ACTA2 (1:200; A5228, Sigma-Aldrich), monoclonal rat-anti-EMCN (1:5, a kind gift from D. Vestweber, MPI Münster; Germany), polyclonal rabbit-anti-CD31 (1:400, 50408-T16, Sino Biological), monoclonal mouse-anti-GFP (1:200, 11814460001 Roche, Sigma-Aldrich) and polyclonal rabbit-anti-GFP (1:250, ab290, Abcam).

Primary antibodies were detected using the following secondary antibodies: biotinylated goat-anti-mouse IgG (1:400; 115-065-003, Dianova), biotinylated goat-anti-rabbit IgG (1:400; 111-065-033, Dianova), biotinylated goat-anti-rat IgG (1:400; 112-065-003, Dianova), biotinylated donkey-anti-goat IgG (1:400; 705-065-003, Dianova), Alexa 488-conjugated goat-anti-rabbit IgG (1:500; A11034, Thermo Fisher Scientific), Alexa 488-conjugated donkey-anti-mouse IgG (1:500; A21202, Thermo Fisher Scientific), Alexa 555-conjugated goat-anti-mouse IgG (1:500; A21422, Thermo Fisher Scientific) and Alexa 555-conjugated goat-anti-mouse IgG (1:500; A21428, Thermo Fisher Scientific).

The signals of NOTCH3, ΔNP63 and EMCN were amplified using the Tyramide Signal Amplification system (NEL702001KT, Perkin Elmer). For detection of JAG1, NOTCH1-3 and RBPJ, the DAB substrate solution (NEL938001EA, Perkin Elmer, Waltham, MA, USA) was used.

For antigen retrieval, paraffin wax-embedded sections were deparaffinized, pressure-cooked for 15 min in antigen unmasking solution (H3300, Vector Laboratories), treated with 3% H_2O_2 /PBS for blocking of endogenous peroxidases, washed in PBST (0.05% Tween-20 in PBS) and incubated in TNB Blocking Buffer (NEL702001KT, Perkin Elmer). Sections were then incubated with primary antibodies at 4°C overnight. Nuclei were stained with 4',6-diamidino-2-phenylindole (DAPI, 6335.1, Carl Roth).

In situ proximity ligation assay

Analysis of direct protein interactions on 5 μm transverse sections of the ureter and dorsal aorta region of wild-type embryos was performed with the proximity ligation assay (Bellucci et al., 2014; Gústafsdóttir et al., 2002) using the Duolink In Situ Red Starter Kit Mouse/Rabbit (DUO92101, Sigma-Aldrich/Merck) applying minor modifications of the manufacturer's instructions, as published before (Lüdtke et al., 2021). Antibody combinations were used and antibody retrieval was performed as described for immunofluorescence analysis. The primary antibody reaction was performed in blocking buffer from the tyramide signal amplification (TSA) system (NEL702001KT, PerkinElmer) overnight at 4°C , containing both corresponding primary antibodies for JAG1 and NOTCH1, NOTCH2 or NOTCH3 in a 1:100 dilution. After three washing steps with PBS/0.1% Tween20 for 5 min, the sections were blocked for 60 min with blocking buffer from the PLA kit and washed three times for 5 min in buffer A from the PLA kit before Duolink PLA probes were applied. Polymerase amplification reaction was performed for 150 min at 37°C .

In situ hybridization analysis

In situ hybridization was carried out on 10 μm paraffin wax-embedded sections essentially as described (Moorman et al., 2001).

Transcriptional profiling by microarrays

Ureters were dissected from male and female control and *Tbx18^{cre/+}; Rbpj^{fl/fl}* embryos. Forty specimens for each sex and genotype were pooled for analysis at E14.5, 12 specimens each for analysis at E18.5 and 10 specimens each for analysis at P4. Total RNA was extracted using peqGOLD RNAPure (732-3312, 30-1010; PeqLab Biotechnologie) and subsequently sent to the Research Core Unit Transcriptomics of Hannover Medical School, where RNA was Cy3-labelled and hybridized to Agilent Whole Mouse Genome Oligo v2 (4 \times 44K) microarrays (G4846A; Agilent Technologies). To identify differentially expressed genes, normalized expression data were filtered using Excel (Microsoft) based on an intensity threshold of 100 and a more than 1.4-fold change in all pools. Microarray data have been deposited in GEO under accession numbers GSE169661, GSE169662 and GSE184597.

Reverse transcription-quantitative polymerase chain reaction (RT-qPCR)

RNA extraction and RT-PCR analysis for *Myocd* and *Foxf1* expression was performed on pools of 10 ureters each of E14.5 control and *Tbx18^{cre/+}; Rbpj^{fl/fl}* embryos, as previously described (Weiss et al., 2019). For all other analyses, we isolated total RNA using TRIzol (15596-018, Thermo Fisher Scientific) and synthesized cDNA from 2.5 µg total RNA applying RevertAid H Minus reverse transcriptase (EP0452, Thermo Fisher Scientific) as described previously (Thiesler et al., 2021). The NCBI tool Primer3 version 4.1 (Untergasser et al., 2012; Ye et al., 2012) was used to design specific primers (Table S16). RT-qPCR of mouse genes was performed in 10 µl 1:2 diluted BIO SyGreen Lo-ROX mix (PCR Biosystems) with 400 nM primers and 1 ng/µl cDNA using a QuantStudio3 PCR system fluorometric thermal cycler (Thermo Fisher Scientific). Each of the three biological replicates represents the average of four technical replicates. Data were processed by QuantStudio data analysis software (version 1.5.1, Thermo Fisher Scientific) using the comparative threshold cycle ($\Delta\Delta C_T$) method with *Gapdh* and *Ppia* as reference genes (Werneburg et al., 2015).

Statistics

Statistical analysis was performed using the unpaired, two-tailed Student's *t*-test (GraphPad Prism version 7.03). Data are mean±s.d. *P*<0.05 was considered significant.

Image documentation

Sections and organ cultures were photographed using a Leica DM5000 microscope with a Leica DFC300FX digital camera or using a Leica DM6000 microscope with Leica DFC350FX digital camera. Urogenital systems were documented using a Leica M420 microscope with a Fujifilm HC-300Z digital camera (Fujifilm Holdings, Minato/Tokyo, Japan). All images were processed in Adobe Photoshop CS4.

Acknowledgements

We thank Doug Melton and Tasuku Honjo for mice; Dietmar Vestweber, Anja-Münster Kühnel, Henry Wedekind and Achim Gossler for antibodies; the Research Core Unit Transcriptomics of Hannover Medical School for microarray analyses; and Patricia Zarnovican for excellent technical support. F.Q. thanks the Hannover Biomedical Research School (HBRS) and the MD/PhD program Molecular Medicine for support. Some data in this study form part of a PhD thesis (J. Kurz, Gottfried Wilhelm Leibniz Universität Hannover, 2021).

Competing interests

The authors declare no competing or financial interests.

Author contributions

Conceptualization: J. Kurz, A.-C.W., A.K.; Methodology: J. Kurz, A.-C.W., H.T., C.R., T.H.L.; Software: M.-O.T.; Validation: J. Kurz, A.-C.W.; Formal analysis: J. Kurz, A.-C.W., H.T., L.D., J. Kaur, C.R., T.H.L., M.-O.T.; Investigation: A.-C.W., L.D., C.R., T.H.L.; Resources: F.Q., I.W., M.-O.T., A.K.; Data curation: J. Kurz, A.-C.W., H.T., L.D., J. Kaur, M.-O.T.; Writing - original draft: A.-C.W., A.K.; Writing - review & editing: J. Kurz, A.-C.W., H.T., F.Q., L.D., J. Kaur, T.H.L., I.W., H.H., M.-O.T., A.K.; Visualization: J. Kurz, A.-C.W., H.T., L.D., J. Kaur; Supervision: H.H., A.K.; Project administration: A.K.; Funding acquisition: H.H., A.K.

Funding

This work was supported by the Deutsche Forschungsgemeinschaft [207786640 (Ki728/9-2), 84948123 (Ki728/7-2) and 171943101 (Ki728/8-2) to A.K.; 432236295 (Hi678/10-1) to H.H.], and by the Horizon 2020 Marie Skłodowska-Curie Actions Initial Training Network (942937) (RENALTRACT to J. Kaur and A.K.).

Data availability

Microarray data have been deposited in GEO under the accession numbers GSE169661, GSE169662 and GSE184597.

References

Airik, R., Trowe, M. O., Foik, A., Farin, H. F., Petry, M., Schuster-Gossler, K., Schweizer, M., Scherer, G., Kist, R. and Kispert, A. (2010). Hydroreteronephrosis due to loss of Sox9-regulated smooth muscle cell differentiation of the ureteric mesenchyme. *Hum. Mol. Genet.* **19**, 4918-4929. doi:10.1093/hmg/ddq426

Aydogdu, N., Rudat, C., Trowe, M. O., Kaiser, M., Ludtke, T. H., Taketo, M. M., Christoffels, V. M., Moon, A. and Kispert, A. (2018). TBX2 and TBX3 act downstream of canonical WNT signaling in patterning and differentiation of the mouse ureteric mesenchyme. *Development* **145**, dev171827. doi:10.1242/dev.171827

Baeten, J. T. and Lilly, B. (2017). Notch signaling in vascular smooth muscle cells. *Adv. Pharmacol.* **78**, 351-382. doi:10.1016/bs.apha.2016.07.002

Bellucci, A., Fiorentini, C., Zaltieri, M., Missale, C. and Spano, P.-F. (2014). The "in situ" proximity ligation assay to probe protein-protein interactions in intact tissues. *Methods Mol. Biol.* **1174**, 397-405. doi:10.1007/978-1-4939-0944-5_27

Bohnenpoll, T., Bettenhausen, E., Weiss, A. C., Foik, A. B., Trowe, M. O., Blank, P., Airik, R. and Kispert, A. (2013). Tbx18 expression demarcates multipotent precursor populations in the developing urogenital system but is exclusively required within the ureteric mesenchymal lineage to suppress a renal stromal fate. *Dev. Biol.* **380**, 25-36. doi:10.1016/j.ydbio.2013.04.036

Bohnenpoll, T., Feraric, S., Nattkemper, M., Weiss, A. C., Rudat, C., Meuser, M., Trowe, M. O. and Kispert, A. (2017a). Diversification of cell lineages in ureter development. *J. Am. Soc. Nephrol.* **28**, 1792-1801. doi:10.1681/ASN.2016080849

Bohnenpoll, T. and Kispert, A. (2014). Ureter growth and differentiation. *Semin. Cell Dev. Biol.* **36**, 21-30. doi:10.1016/j.semcdb.2014.07.014

Bohnenpoll, T., Weiss, A. C., Labuhn, M., Ludtke, T. H., Trowe, M. O. and Kispert, A. (2017b). Retinoic acid signaling maintains epithelial and mesenchymal progenitors in the developing mouse ureter. *Sci. Rep.* **7**, 14803. doi:10.1038/s41598-017-14790-2

Bohnenpoll, T., Wittern, A. B., Mamo, T. M., Weiss, A. C., Rudat, C., Kleppa, M. J., Schuster-Gossler, K., Wojahn, I., Ludtke, T. H., Trowe, M. O. et al. (2017c). A SHH-FOXF1-BMP4 signaling axis regulating growth and differentiation of epithelial and mesenchymal tissues in ureter development. *PLoS Genet.* **13**, e1006951. doi:10.1371/journal.pgen.1006951

Bray, S. and Bernard, F. (2010). Notch targets and their regulation. *Curr. Top. Dev. Biol.* **92**, 253-275. doi:10.1016/S0070-2153(10)92008-5

Caubit, X., Lye, C. M., Martin, E., Core, N., Long, D. A., Vola, C., Jenkins, D., Garratt, A. N., Skaer, H., Woolf, A. S. et al. (2008). Teashirt 3 is necessary for ureteral smooth muscle differentiation downstream of SHH and BMP4. *Development* **135**, 3301-3310. doi:10.1242/dev.022442

Cheng, H. T., Miner, J. H., Lin, M., Tansey, M. G., Roth, K. and Kopan, R. (2003). Gamma-secretase activity is dispensable for mesenchyme-to-epithelium transition but required for podocyte and proximal tubule formation in developing mouse kidney. *Development* **130**, 5031-5042. doi:10.1242/dev.00697

Creemers, E. E., Sutherland, L. B., McAnally, J., Richardson, J. A. and Olson, E. N. (2006). Myocardin is a direct transcriptional target of Mef2, Tead and Foxo proteins during cardiovascular development. *Development* **133**, 4245-4256. doi:10.1242/dev.02610

Donadon, M. and Santoro, M. M. (2021). The origin and mechanisms of smooth muscle cell development in vertebrates. *Development* **148**, dev197384. doi:10.1242/dev.197384

Etchevers, H. C., Vincent, C., Le Douarin, N. M. and Couly, G. F. (2001). The cephalic neural crest provides pericytes and smooth muscle cells to all blood vessels of the face and forebrain. *Development* **128**, 1059-1068.

Feng, X., Krebs, L. T. and Gridley, T. (2010). Patent ductus arteriosus in mice with smooth muscle-specific Jag1 deletion. *Development* **137**, 4191-4199. doi:10.1242/dev.052043

Fischer, A., Schumacher, N., Maier, M., Sendtner, M. and Gessler, M. (2004). The Notch target genes Hey1 and Hey2 are required for embryonic vascular development. *Genes Dev.* **18**, 901-911.

Fouillade, C., Monet-Leprêtre, M., Baron-Menguy, C. and Joutel, A. (2012). Notch signalling in smooth muscle cells during development and disease. *Cardiovasc. Res.* **95**, 138-146. doi:10.1093/cvr/cvs019

Ghosh, S., Paez-Cortez, J. R., Boppidi, K., Vasconcelos, M., Roy, M., Cardoso, W., Ai, X. and Fine, A. (2011). Activation dynamics and signaling properties of Notch3 receptor in the developing pulmonary artery. *J. Biol. Chem.* **286**, 22678-22687. doi:10.1074/jbc.M111.241224

Grieskamp, T., Rudat, C., Ludtke, T. H., Norden, J. and Kispert, A. (2011). Notch signaling regulates smooth muscle differentiation of epicardium-derived cells. *Circ. Res.* **108**, 813-823. doi:10.1161/CIRCRESAHA.110.228809

Guimaraes-Camboa, N., Cattaneo, P., Sun, Y., Moore-Morris, T., Gu, Y., Dalton, N. D., Rockenstein, N. E., Masliah, E., Peterson, K. L., Stallcup, W. B. et al. (2017). Pericytes of multiple organs do not behave as mesenchymal stem cells in Vivo. *Cell Stem Cell* **20**, 345-359.e5. doi:10.1016/j.stem.2016.12.006

Gústafsdóttir, M., Östman, A. and Landegren, U. (2002). Protein detection using proximity-dependent DNA ligation assays. *Nat. Biotechnol.* **20**, 473-477. doi:10.1038/nbt0502-473

Henrique, D. and Schweisguth, F. (2019). Mechanisms of Notch signaling: a simple logic deployed in time and space. *Development* **146**, dev172148. doi:10.1242/dev.172148

High, F. A., Zhang, M., Proweller, A., Tu, L., Parmacek, M. S., Pear, W. S. and Epstein, J. A. (2007). An essential role for Notch in neural crest during cardiovascular development and smooth muscle differentiation. *J. Clin. Invest.* **117**, 353-363. doi:10.1172/JCI30070

- High, F. A., Lu, M. M., Pear, W. S., Loomes, K. M., Kaestner, K. H. and Epstein, J. A. (2008). Endothelial expression of the Notch ligand Jagged1 is required for vascular smooth muscle development. *Proc. Natl. Acad. Sci. USA* **105**, 1955-1959. doi:10.1073/pnas.0709663105
- Hoglund, V. J. and Majesky, M. W. (2012). Patterning the artery wall by lateral induction of Notch signaling. *Circulation* **125**, 212-215. doi:10.1161/CIRCULATIONAHA.111.075937
- Huang da, W., Sherman, B. T. and Lempicki, R. A. (2009). Systematic and integrative analysis of large gene lists using DAVID bioinformatics resources. *Nat. Protoc.* **4**, 44-57. doi:10.1038/nprot.2008.211
- Jarriault, S., Brou, C., Logeat, F., Schroeter, E. H., Kopan, R. and Israel, A. (1995). Signalling downstream of activated mammalian Notch. *Nature* **377**, 355-358. doi:10.1038/377355a0
- Joutel, A., Andreux, F., Gaulis, S., Domenga, V., Cecillon, M., Battail, N., Piga, N., Chapon, F., Godfrain, C. and Tournier-Lasserre, E. (2000). The ectodomain of the Notch3 receptor accumulates within the cerebrovasculature of CADASIL patients. *J. Clin. Invest.* **105**, 597-605. doi:10.1172/JCI8047
- Kim, E. E., Shekhar, A., Lu, J., Lin, X., Liu, F. Y., Zhang, J., Delmar, M. and Fishman, G. I. (2014). PCP4 regulates Purkinje cell excitability and cardiac rhythmicity. *J. Clin. Invest.* **124**, 5027-5036. doi:10.1172/JCI77495
- Kohl, S., Habbig, S., Weber, L. T. and Liebau, M. C. (2021). Molecular causes of congenital anomalies of the kidney and urinary tract (CAKUT). *Mol. Cell Pediatr* **8**, 2. doi:10.1186/s40348-021-00112-0
- Kopan, R. (2012). Notch signaling. *Cold Spring Harb. Perspect Biol.* **4**, a011213. doi:10.1101/cshperspect.a011213
- Kovall, R. A., Gebelein, B., Sprinzak, D. and Kopan, R. (2017). The Canonical Notch Signaling Pathway: Structural and Biochemical Insights into Shape, Sugar, and Force. *Dev. Cell* **41**, 228-241. doi:10.1016/j.devcel.2017.04.001
- Liu, H., Kennard, S. and Lilly, B. (2009). NOTCH3 expression is induced in mural cells through an autoregulatory loop that requires endothelial-expressed JAGGED1. *Circ. Res.* **104**, 466-475. doi:10.1161/CIRCRESAHA.108.184846
- Liu, H., Zhang, W., Kennard, S., Caldwell, R. B. and Lilly, B. (2010). Notch3 is critical for proper angiogenesis and mural cell investment. *Circ. Res.* **107**, 860-870. doi:10.1161/CIRCRESAHA.110.218271
- Lüdtke, T. H., Wojahn, I., Kleppa, M.-J., Schierstaedt, J., Christoffels, V. M., Künzler, P. and Kispert, A. (2021). Combined genomic and proteomic approaches reveal DNA binding sites and interaction partners of TBX2 in the developing lung. *Respir. Res.* **22**, 85. doi:10.1186/s12931-021-01679-y
- Mack, C. P. (2011). Signaling mechanisms that regulate smooth muscle cell differentiation. *Arterioscler. Thromb. Vasc. Biol.* **31**, 1495-1505. doi:10.1161/ATVBAHA.110.221135
- Mamo, T. M., Wittern, A. B., Kleppa, M. J., Bohnenpoll, T., Weiss, A. C. and Kispert, A. (2017). BMP4 uses several different effector pathways to regulate proliferation and differentiation in the epithelial and mesenchymal tissue compartments of the developing mouse ureter. *Hum. Mol. Genet.* **26**, 3553-3563. doi:10.1093/hmg/ddx242
- Manderfield, L. J., High, F. A., Engleka, K. A., Liu, F., Li, L., Rentschler, S. and Epstein, J. A. (2012). Notch activation of Jagged1 contributes to the assembly of the arterial wall. *Circulation* **125**, 314-323. doi:10.1161/CIRCULATIONAHA.111.047159
- Moorman, A. F., Houweling, A. C., de Boer, P. A. and Christoffels, V. M. (2001). Sensitive nonradioactive detection of mRNA in tissue sections: novel application of the whole-mount in situ hybridization protocol. *J. Histochem. Cytochem.* **49**, 1-8. doi:10.1177/002215540104900101
- Morgan, S. M., Samulowitz, U., Darley, L., Simmons, D. L. and Vestweber, D. (1999). Biochemical characterization and molecular cloning of a novel endothelial-specific sialomucin. *Blood* **93**, 165-175. doi:10.1182/blood.V93.1.165
- Murtaugh, L. C., Stanger, B. Z., Kwan, K. M. and Melton, D. A. (2003). Notch signaling controls multiple steps of pancreatic differentiation. *Proc. Natl. Acad. Sci. USA* **100**, 14920-14925. doi:10.1073/pnas.2436557100
- Muzumdar, M. D., Tasic, B., Miyamichi, K., Li, L. and Luo, L. (2007). A global double-fluorescent Cre reporter mouse. *Genesis* **45**, 593-605. doi:10.1002/dvg.20335
- Norman, C., Runswick, M., Pollock, R. and Treisman, R. (1988). Isolation and properties of cDNA clones encoding SRF, a transcription factor that binds to the c-fos serum response element. *Cell* **55**, 989-1003. doi:10.1016/0092-8674(88)90244-9
- Rentschler, S., Yen, A., Lu, J., Petrenko, N., Lu, M., Manderfield, L., Patel, V., Fishman, G. and Epstein, J. (2012). Myocardial Notch signaling reprograms cardiomyocytes to a conduction-like phenotype. *Circulation* **126**, 1058-1066. doi:10.1161/CIRCULATIONAHA.112.103390
- Shi, N. and Chen, S. Y. (2016). Smooth muscle cell differentiation: model systems, regulatory mechanisms, and vascular diseases. *J. Cell. Physiol.* **231**, 777-787. doi:10.1002/jcp.25208
- Tanigaki, K., Han, H., Yamamoto, N., Tashiro, K., Ikegawa, M., Kuroda, K., Suzuki, A., Nakano, T. and Honjo, T. (2002). Notch-RBP-J signaling is involved in cell fate determination of marginal zone B cells. *Nat. Immunol.* **3**, 443-450. doi:10.1038/ni793
- Thiesler, H., Beimdick, J. and Hildebrandt, H. (2021). Polysialic acid and Siglec-E orchestrate negative feedback regulation of microglia activation. *Cell. Mol. Life Sci.* **78**, 1637-1653. doi:10.1007/s00018-020-03601-z
- Trowe, M. O., Shah, S., Petry, M., Airik, R., Schuster-Gossler, K., Kist, R. and Kispert, A. (2010). Loss of Sox9 in the periotic mesenchyme affects mesenchymal expansion and differentiation, and epithelial morphogenesis during cochlea development in the mouse. *Dev. Biol.* **342**, 51-62. doi:10.1016/j.ydbio.2010.03.014
- Trowe, M. O., Airik, R., Weiss, A. C., Farin, H. F., Foik, A. B., Bettenhausen, E., Schuster-Gossler, K., Taketo, M. M. and Kispert, A. (2012). Canonical Wnt signaling regulates smooth muscle precursor development in the mouse ureter. *Development* **139**, 3099-3108. doi:10.1242/dev.077388
- Untergasser, A., Cutcutache, I., Koressaar, T., Ye, J., Faircloth, B. C., Remm, M. and Rozen, S. G. (2012). Primer3-new capabilities and interfaces. *Nucleic Acids Res.* **40**, e115.
- Volz, K. S., Jacobs, A. H., Chen, H. I., Poduri, A., McKay, A. S., Riordan, D. P., Kofler, N., Kitajewski, J., Weissman, I. and Red-Horse, K. (2015). Pericytes are progenitors for coronary artery smooth muscle. *Elife* **4**, e10036. doi:10.7554/eLife.10036
- Walker, M. A., Chavez, J., Villet, O., Tang, X., Keller, A., Bruce, J. E. and Tian, R. (2021). Acetylation of muscle creatine kinase negatively impacts high-energy phosphotransfer in heart failure. *JCI Insight* **6**, e144301. doi:10.1172/jci.insight.144301
- Wang, D. Z. and Olson, E. N. (2004). Control of smooth muscle development by the myocardin family of transcriptional coactivators. *Curr. Opin. Genet. Dev.* **14**, 558-566. doi:10.1016/j.gde.2004.08.003
- Wang, Q., Zhao, N., Kennard, S. and Lilly, B. (2012). Notch2 and Notch3 function together to regulate vascular smooth muscle development. *PLoS ONE* **7**, e37365. doi:10.1371/journal.pone.0037365
- Wei, B. and Jin, J. P. (2016). TNNT1, TNNT2, and TNNT3: Isoform genes, regulation, and structure-function relationships. *Gene* **582**, 1-13. doi:10.1016/j.gene.2016.01.006
- Weiss, A. C., Bohnenpoll, T., Kurz, J., Blank, P., Airik, R., Lüdtke, T. H., Kleppa, M. J., Deuper, L., Kaiser, M., Mamo, T. M. et al. (2019). Delayed onset of smooth muscle cell differentiation leads to hydroureter formation in mice with conditional loss of the zinc finger transcription factor gene Gata2 in the ureteric mesenchyme. *J. Pathol.* **248**, 452-463. doi:10.1002/path.5270
- Werneburg, S., Buettner, F. F., Mühlenhoff, M. and Hildebrandt, H. (2015). Polysialic acid modification of the synaptic cell adhesion molecule SynCAM 1 in human embryonic stem cell-derived oligodendrocyte precursor cells. *Stem Cell Res* **14**, 339-346. doi:10.1016/j.scr.2015.03.001
- Wolf, A. S. and Davies, J. A. (2013). Cell biology of ureter development. *J. Am. Soc. Nephrol.* **24**, 19-25. doi:10.1681/ASN.2012020127
- Wolf, A. S., Lopes, F. M., Ranjzad, P. and Roberts, N. A. (2019). Congenital disorders of the human urinary tract: recent insights from genetic and molecular studies. *Front. Pediatr.* **7**, 136. doi:10.3389/fped.2019.00136
- Ye, J., Coulouris, G., Zaretskaya, I., Cutcutache, I., Rozen, S. and Madden, T. L. (2012). Primer-BLAST: a tool to design target-specific primers for polymerase chain reaction. *BMC Bioinformatics* **13**, 134. doi:10.1186/1471-2105-13-134
- Yoshida, T., Sinha, S., Dandre, F., Wamhoff, B. R., Hoofnagle, M. H., Kremer, B. E., Wang, D. Z., Olson, E. N. and Owens, G. K. (2003). Myocardin is a key regulator of CArG-dependent transcription of multiple smooth muscle marker genes. *Circ. Res.* **92**, 856-864. doi:10.1161/01.RES.0000068405.49081.09
- Yu, J., Carroll, T. J. and McMahon, A. P. (2002). Sonic hedgehog regulates proliferation and differentiation of mesenchymal cells in the mouse metanephric kidney. *Development* **129**, 5301-5312. doi:10.1242/dev.129.22.5301

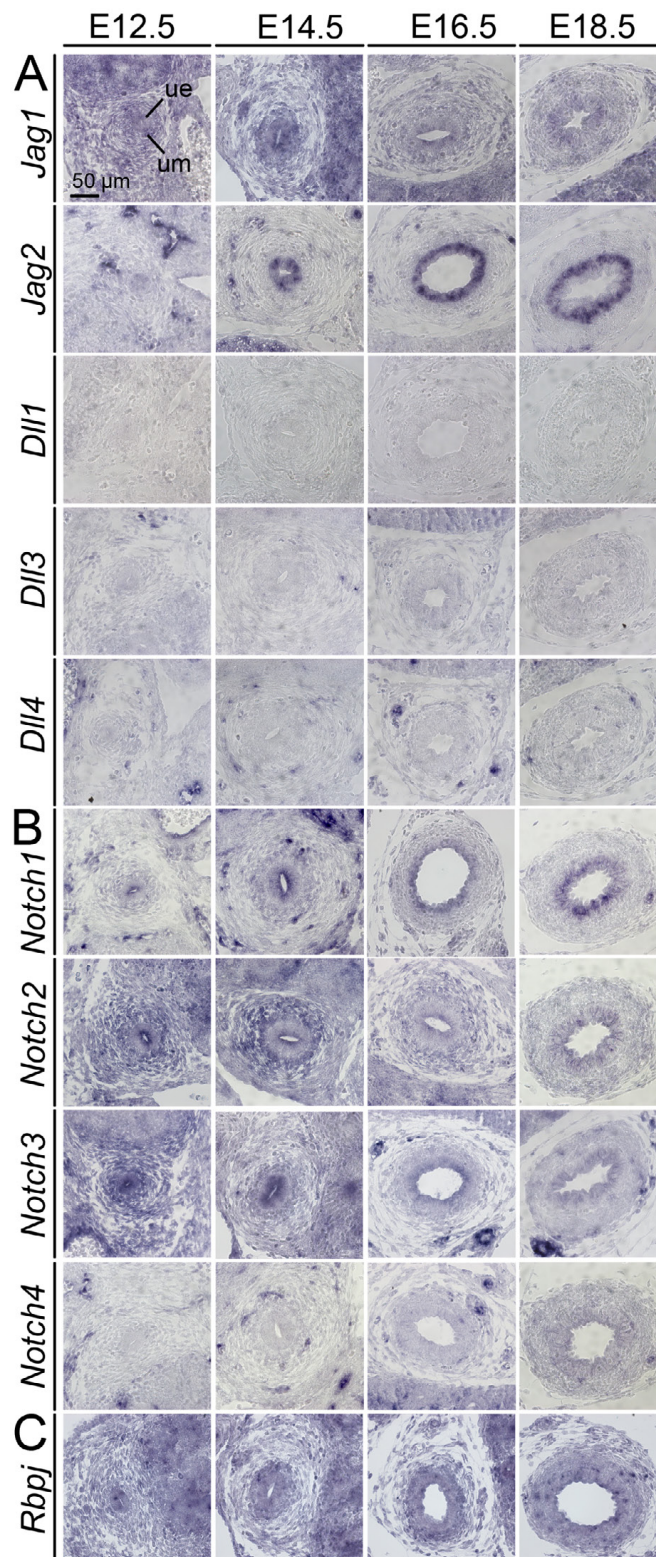


Fig. S1. Notch signaling components are expressed during murine ureter development. (A-C) RNA *in situ* hybridization analysis on transverse sections of the proximal ureter for expression of genes encoding Notch ligands (A), Notch receptors (B) and the signaling mediator *Rbpj* (C). $n \geq 3$ for all probes and stages. ue, ureteric epithelium; um, ureteric mesenchyme.

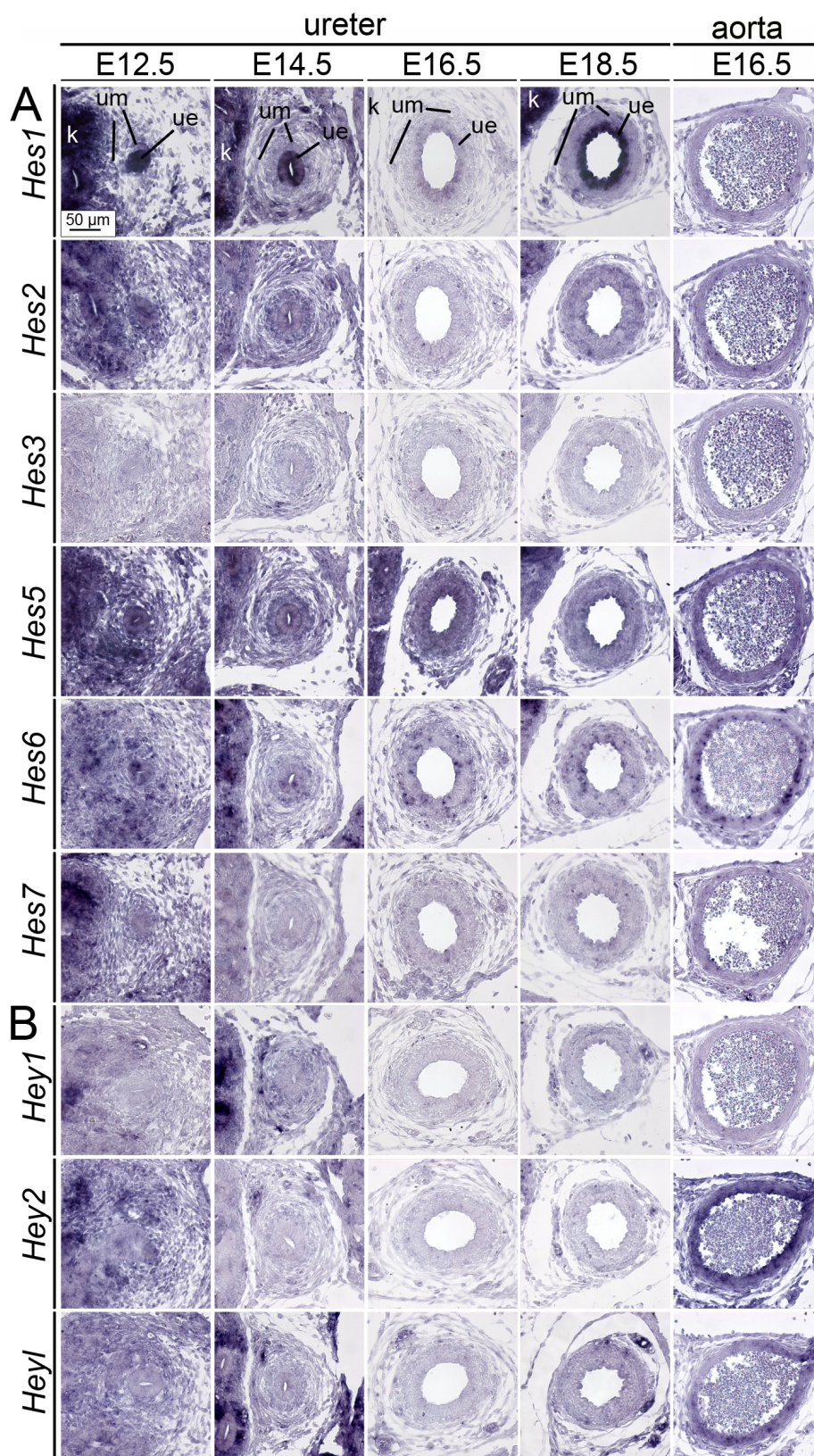


Fig. S2. Notch target genes are expressed during murine ureter development. (A,B) RNA *in situ* hybridization analysis on transverse sections of the proximal ureter and the dorsal aorta for expression of *Hes* (A) and *Hey* (B) genes. $n \geq 3$ for all probes and stages. k, kidney; ue, ureteric epithelium; um, ureteric mesenchyme.

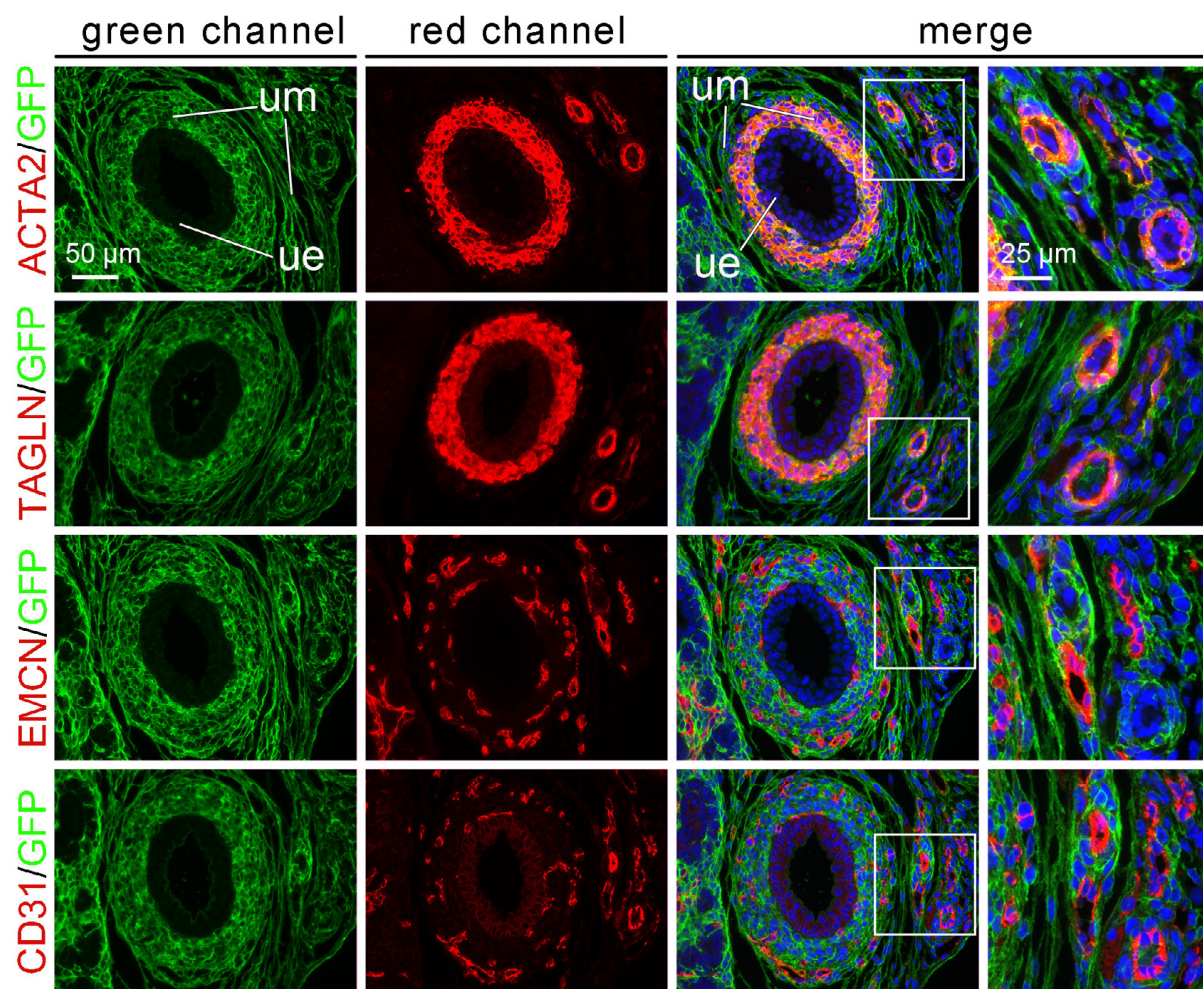


Fig. S3. Lineage analysis of *Tbx18*⁺ descendants in the ureter. Co-immunofluorescence analysis on transverse sections of the proximal ureter of E18.5 *Tbx18*^{cre/+}; *R26*^{mTmG/+} embryos for expression of the lineage marker GFP and of differentiation markers for SMCs (ACTA2, TAGLN) and endothelial cells (EMCN, CD31). Shown are the green channel for GFP expression (first column), the red channel for the differentiation marker (second column), and a merge of the two channels (third and fourth column). The fourth column shows higher magnification images of the regions marked by a white square in the third column, which contain vessels with SMC investment. n=5 for all markers. Note that visceral and vascular SMCs arise from *Tbx18*⁺ mesenchymal progenitors whereas endothelial cells are of a different origin. ue, ureteric epithelium; um, ureteric mesenchyme.

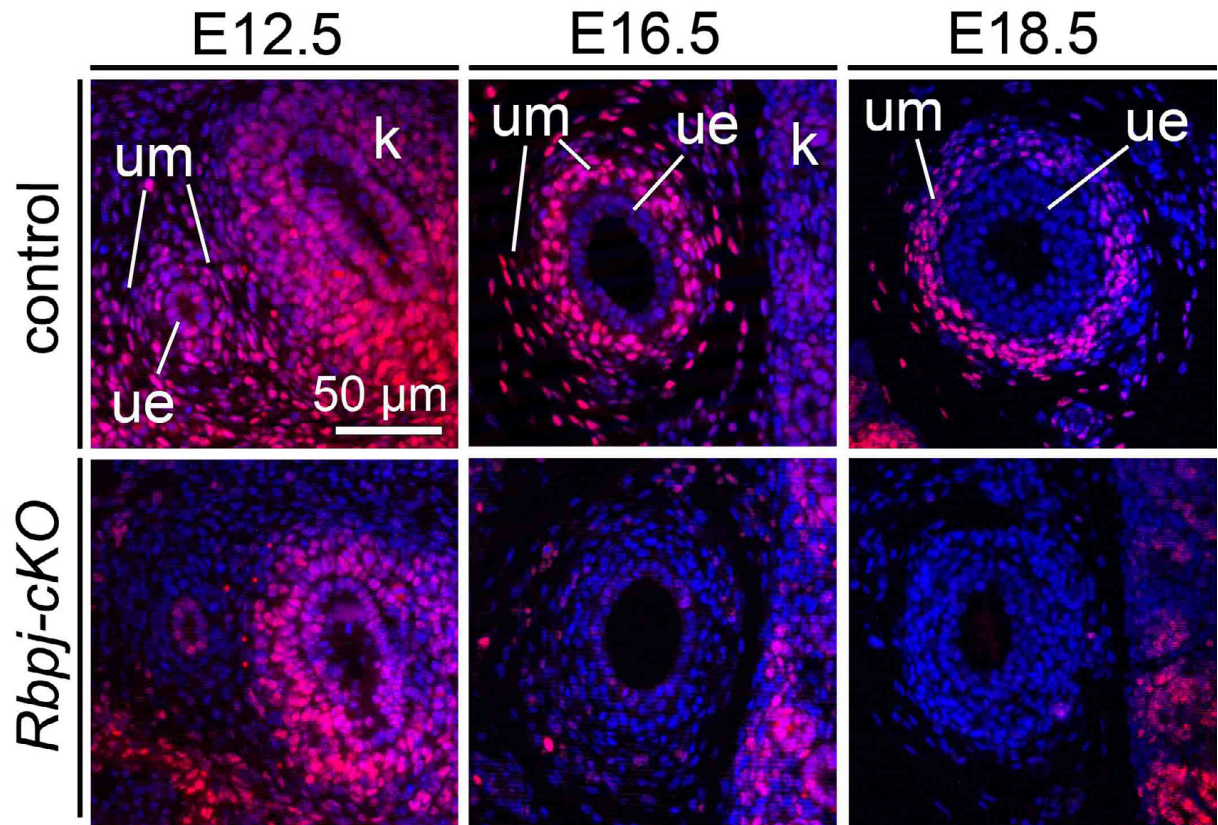


Fig. S4. Loss of RBPJ expression in the UM of *Rbpj-cKO* embryos. Immunofluorescence analysis of RBPJ expression on transverse sections of the proximal region of control and *Rbpj-cKO* ureters at E12.5, E16.5 and E18.5; n=4 for both genotypes and stages. k, kidney; ue, ureteric epithelium; um, ureteric mesenchyme.

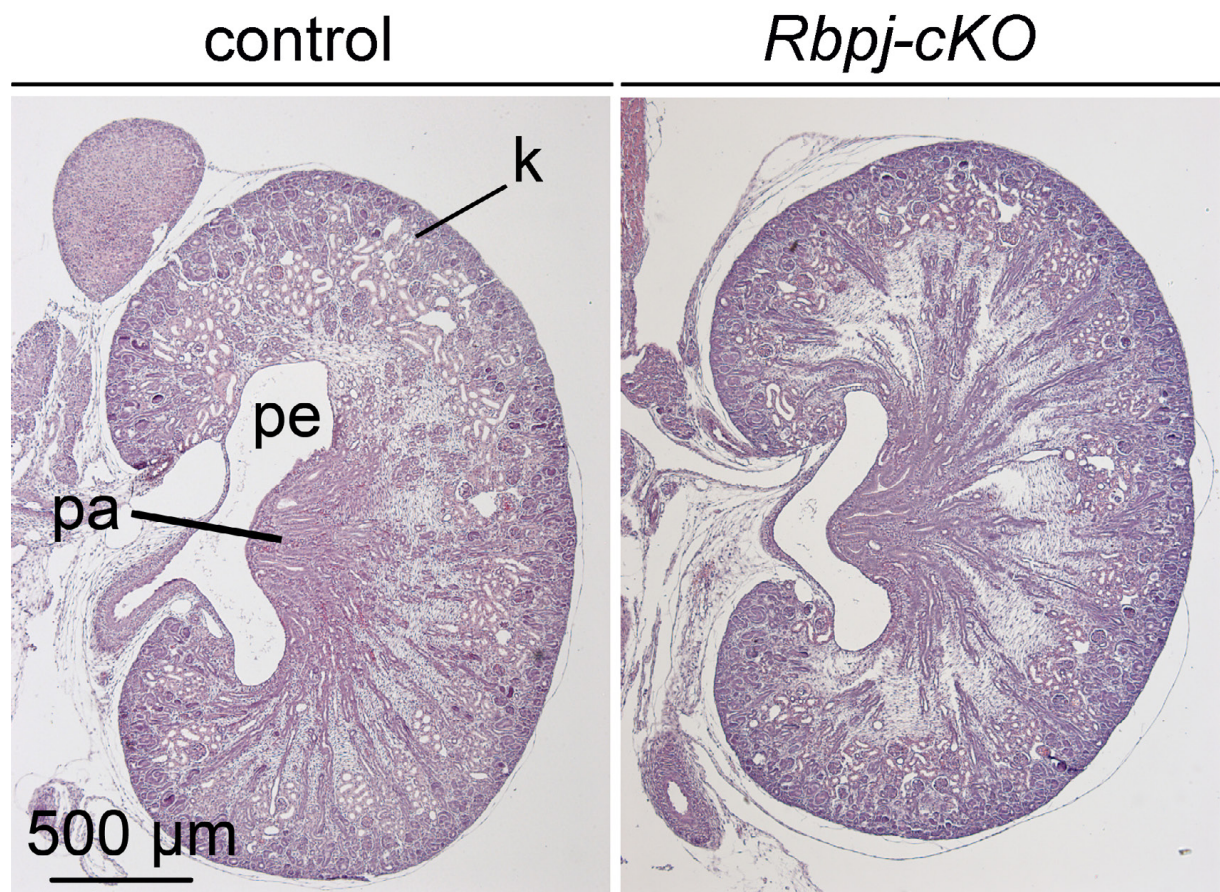


Fig. S5. Renal histology is unaltered in *Rbpj-cKO* embryos at E18.5. Hematoxylin and eosin staining of sagittal sections of control and *Rbpj-cKO* kidneys at E18.5. n=3 for both genotypes. k, kidney; pa, papilla; pe, pelvis;

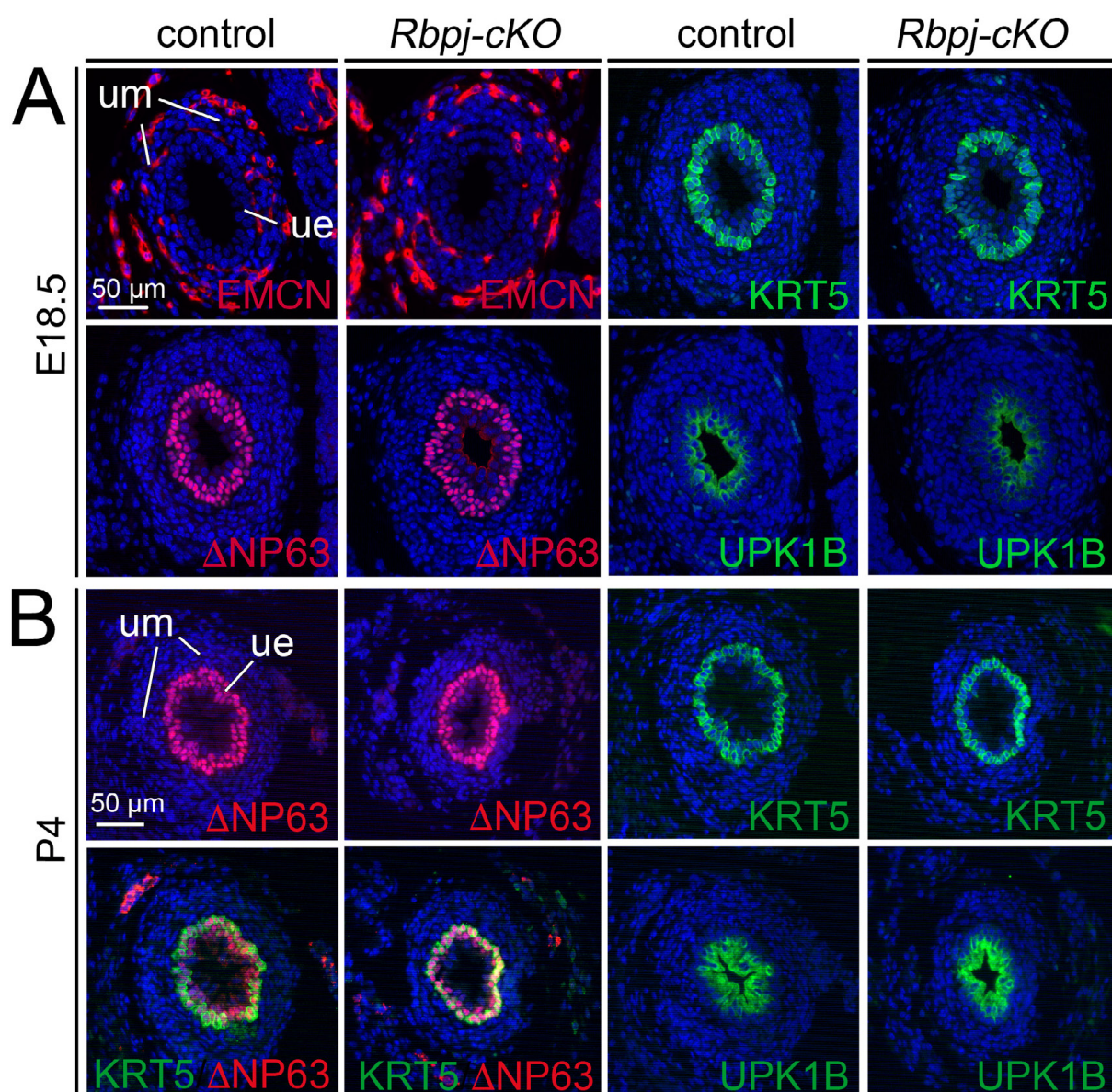


Fig. S6. *Rbpj-cKO* ureters do not show urothelial defects at E18.5 and P4. (A,B) Immunofluorescence analysis for endothelial (EMCN) and urothelial (KRT5, Δ NP63, UPK1B) differentiation markers on proximal sections of E18.5 (**A**) and P4 ureters (**B**). Nuclei (blue) are counterstained with DAPI. KRT5, Δ NP63 and UPK1B combinatorially mark basal cells (KRT5⁺ Δ NP63⁺UPK1B⁻), intermediate cells (KRT5⁻ Δ NP63⁺UPK1B⁺) and superficial cells (KRT5⁻ Δ NP63⁻UPK1B⁺). n=4 for each marker, genotype and stage. ue, ureteric epithelium; um, ureteric mesenchyme.

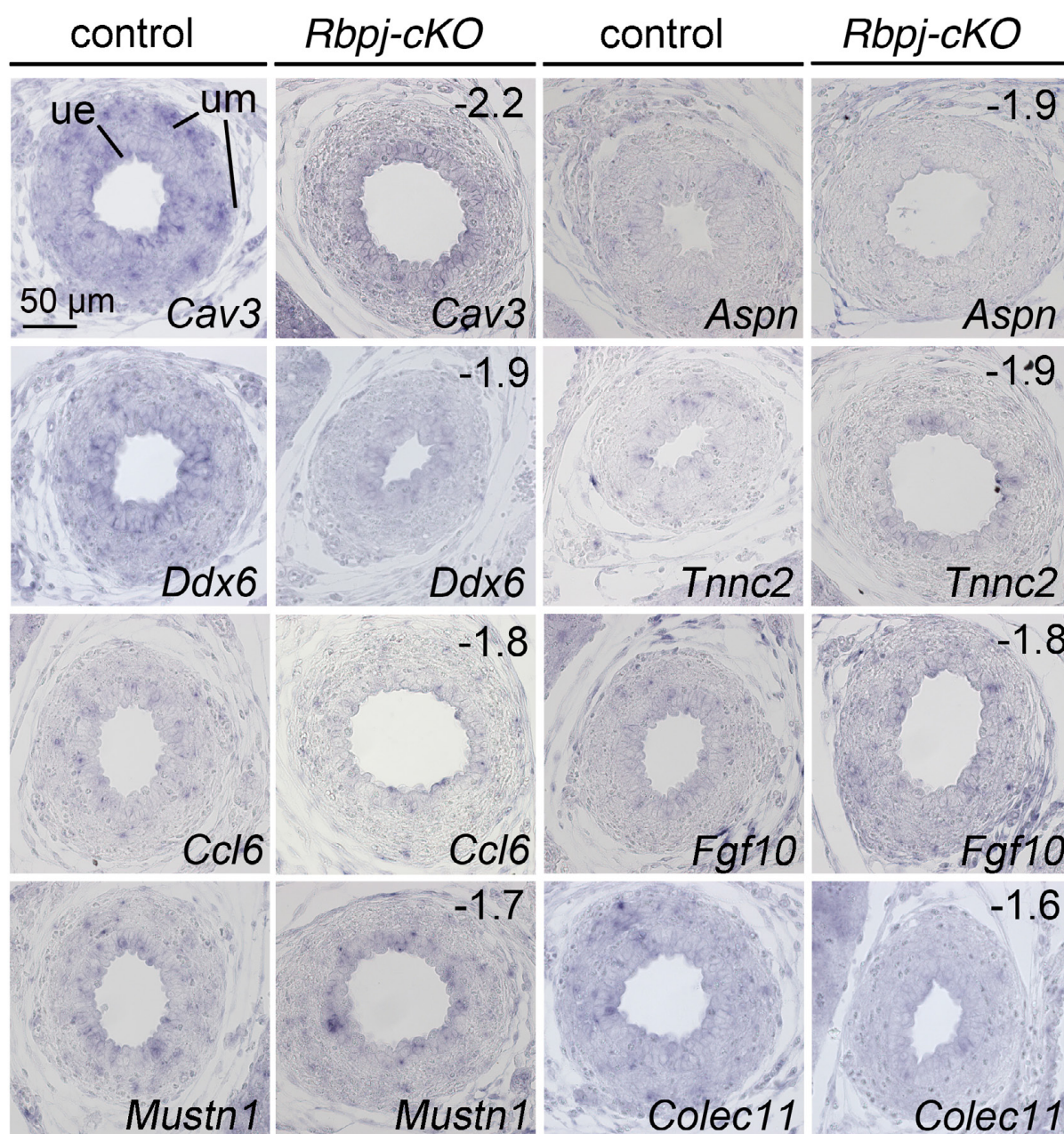


Fig. S7. RNA *in situ* hybridization analysis of candidate genes with decreased expression in microarrays of E18.5 *Rbpj-cKO* ureters. RNA *in situ* hybridization analysis of selected candidate genes with decreased expression in microarrays of E18.5 *Rbpj-cKO* ureters was performed on transverse sections of the proximal ureter region of control and *Rbpj-cKO* embryos at E18.5. Probes, genotypes and fold changes in the microarray are as indicated. $n \geq 3$ for all probes and genotypes. ue, ureteric epithelium; um, ureteric mesenchyme.

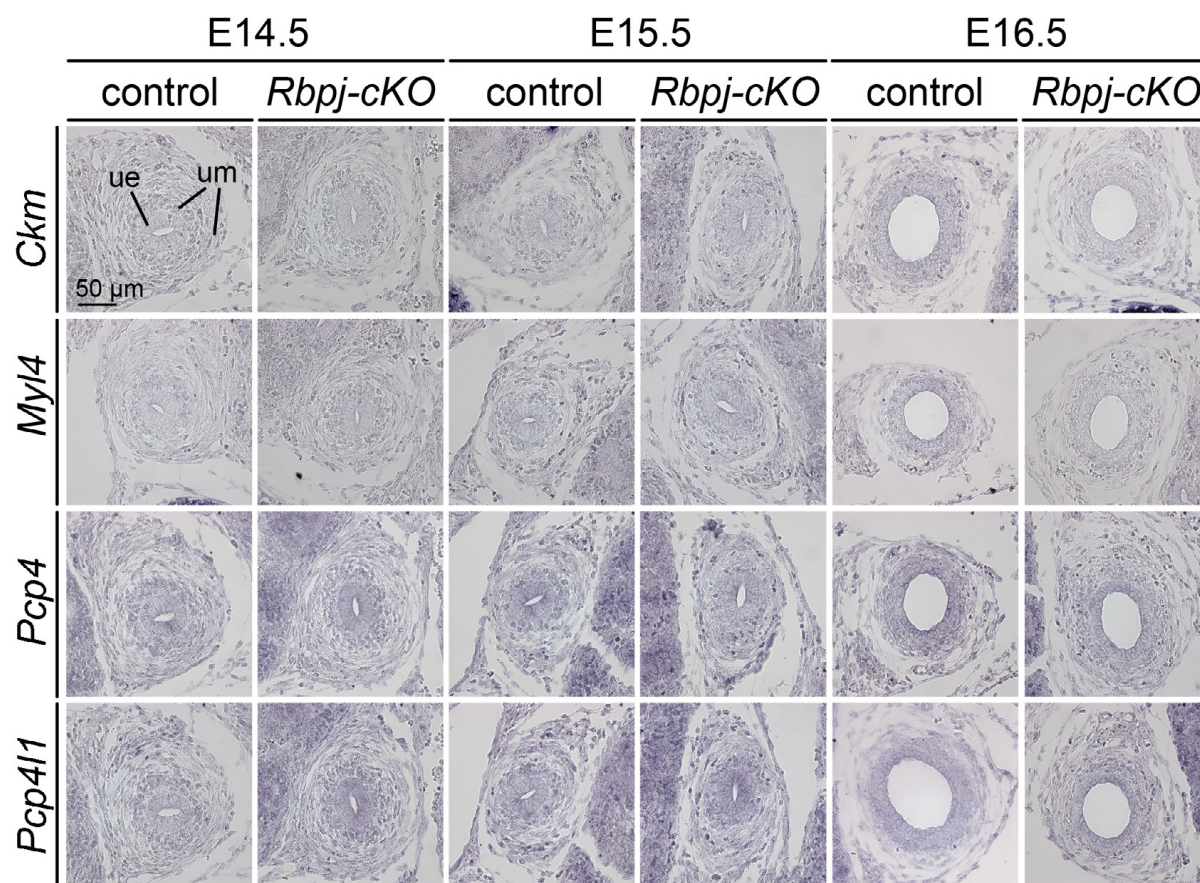


Fig. S8. RNA *in situ* hybridization analysis of selected SMC genes in ureter development. RNA *in situ* hybridization analysis of selected SMC genes was performed on transverse sections of the proximal ureter region of control and *Rbpj-cKO* embryos at E14.5, E15.5 and E16.5. $n \geq 3$ for all probes and genotypes. ue, ureteric epithelium; um, ureteric mesenchyme.

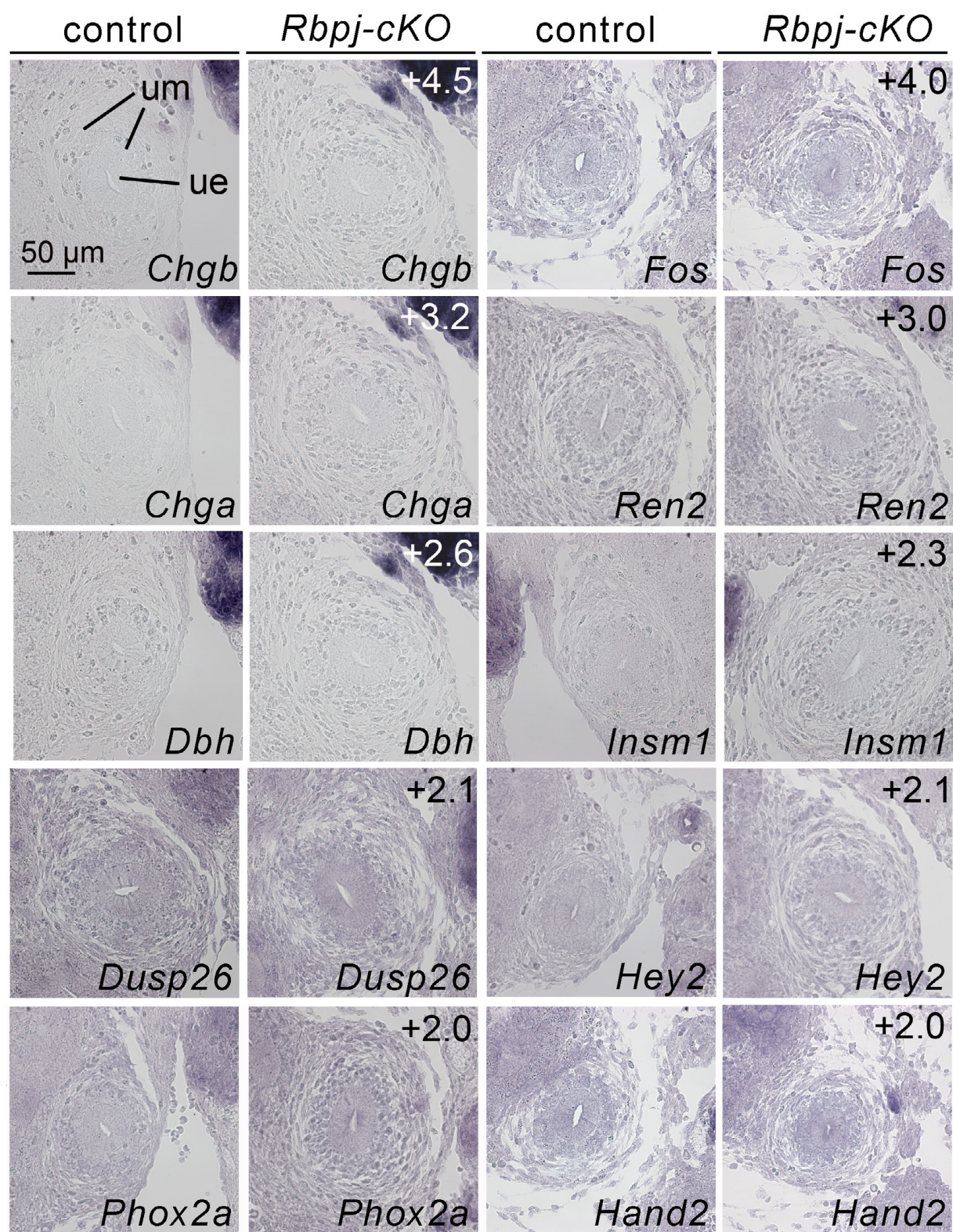


Fig. S9. RNA *in situ* hybridization analysis of candidate genes with increased expression in microarrays of E14.5 *Rbpj-cKO* ureters. RNA *in situ* hybridization analysis of selected candidate genes with increased expression in microarrays of E14.5 *Rbpj-cKO* ureters was performed on transverse sections of the proximal ureter region of E14.5 control and *Rbpj-cKO* embryos. Numbers refer to fold increase in the microarray. $n \geq 3$ for all probes and genotypes. ue, ureteric epithelium; um, ureteric mesenchyme.

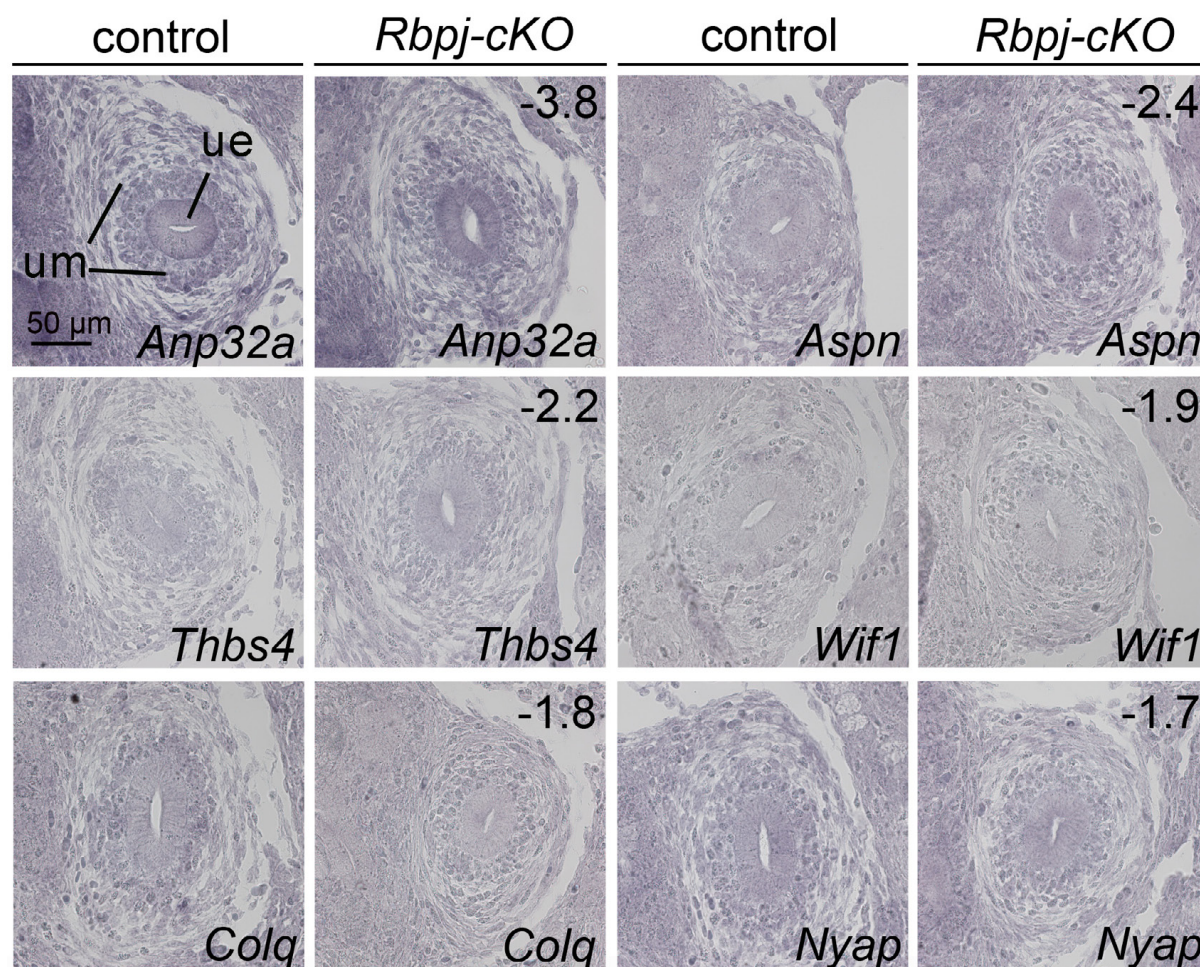


Fig. S10. RNA *in situ* hybridization analysis of candidate genes with decreased expression in microarrays of E14.5 *Rbpj-cKO* ureters. RNA *in situ* hybridization analysis of selected candidate genes with decreased expression in microarrays of E14.5 *Rbpj-cKO* ureters was performed on transverse sections of the proximal ureter region of E14.5 control and *Rbpj-cKO* embryos. Numbers refer to fold change in the microarray. $n \geq 3$ for all probes and genotypes. ue, ureteric epithelium; um, ureteric mesenchyme.

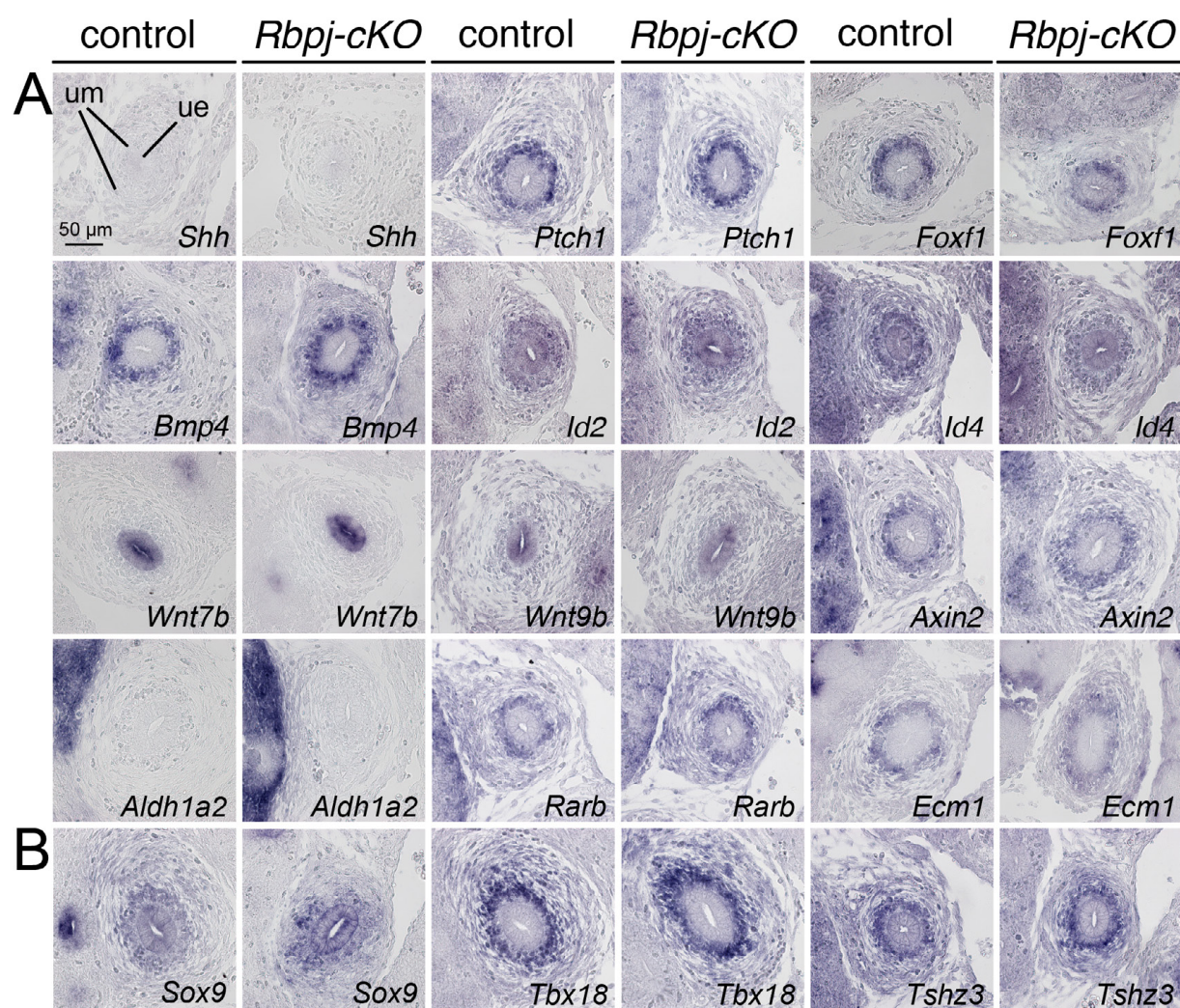


Fig. S11. Signaling pathways and transcription factor genes relevant for SMC differentiation are unchanged in their activity/expression in *Rbpj-cKO* ureters at E14.5. (A,B) RNA *in situ* hybridization analysis of expression of *Shh*, its target gene *Ptch1* and its effector gene *Foxf1*; of *Bmp4*, its target genes *Id2* and *Id4*; of *Wnt7b* and *Wnt9b*, and the WNT target gene *Axin2*; of the gene encoding the RA synthesizing enzyme *Aldh1a2*, and the targets of RA signaling activity in the UM, *Rarb* and *Ecm1* (A) and of the transcription factor genes *Sox9*, *Tbx18* and *Tshz3* (B) on transverse sections of the proximal ureter of control and *Rbpj-cKO* embryos at E14.5. Genotypes, probes and fold change in the microarray are shown. $n \geq 3$ for all probes and genotypes. ue, ureteric epithelium; um, ureteric mesenchyme.

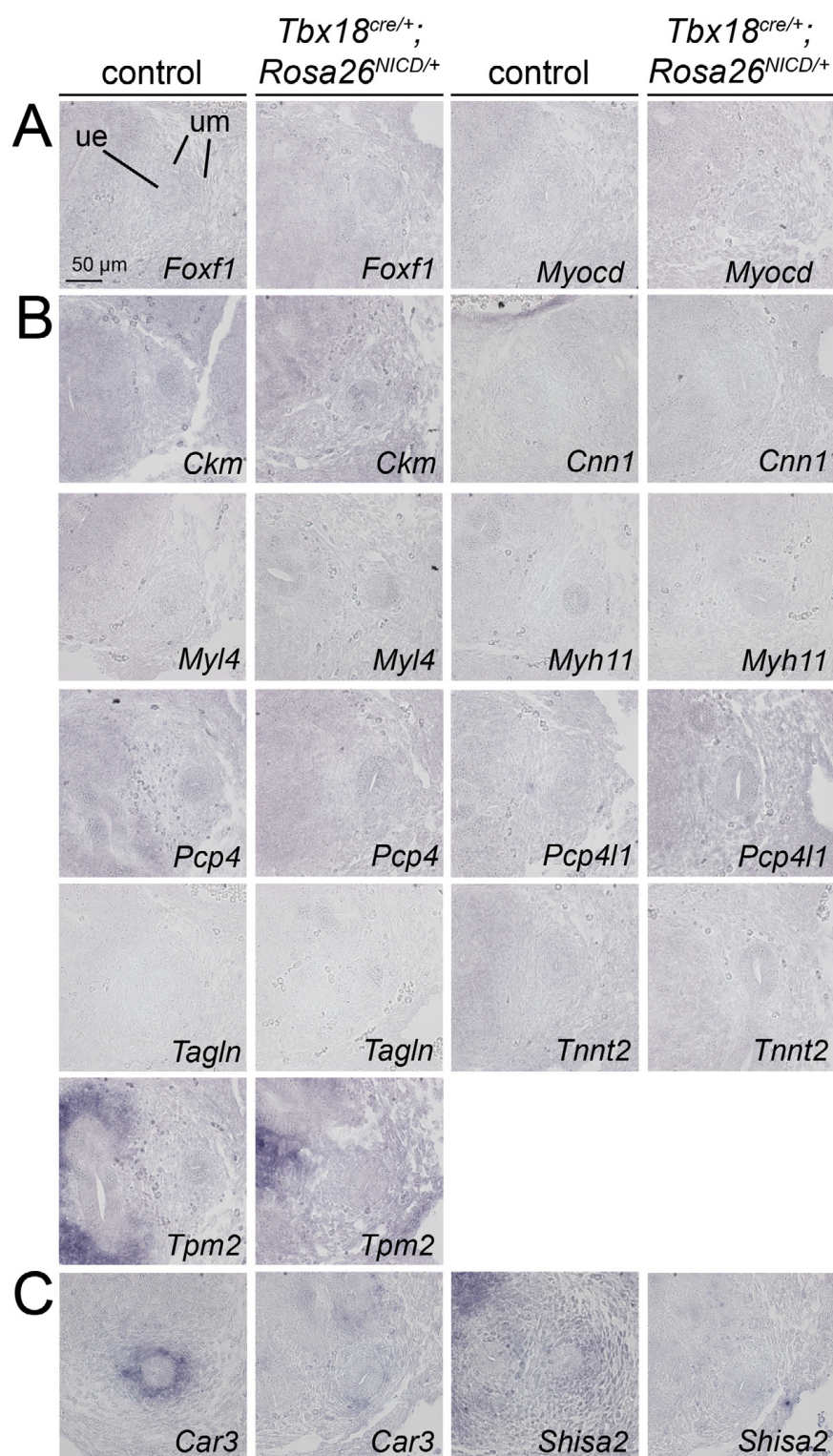


Fig. S12. Ectopic expression of the Notch1 intracellular domain (N1CD) does not induce premature expression of SMC regulatory and structural genes in the UM. (A) RNA *in situ* hybridization analysis on transverse sections of E12.5 control and *Tbx18^{cre/+};
Rosa26^{N1CD/+}* ureters for expression of SMC regulatory genes (A), SMC structural genes (B) and genes with reduced expression in E14.5 *Rbpj-cKO* microarray, *Car3* and *Shisa2* (C); n=3 for all probes and genotypes. ue, ureteric epithelium; um, ureteric mesenchyme.

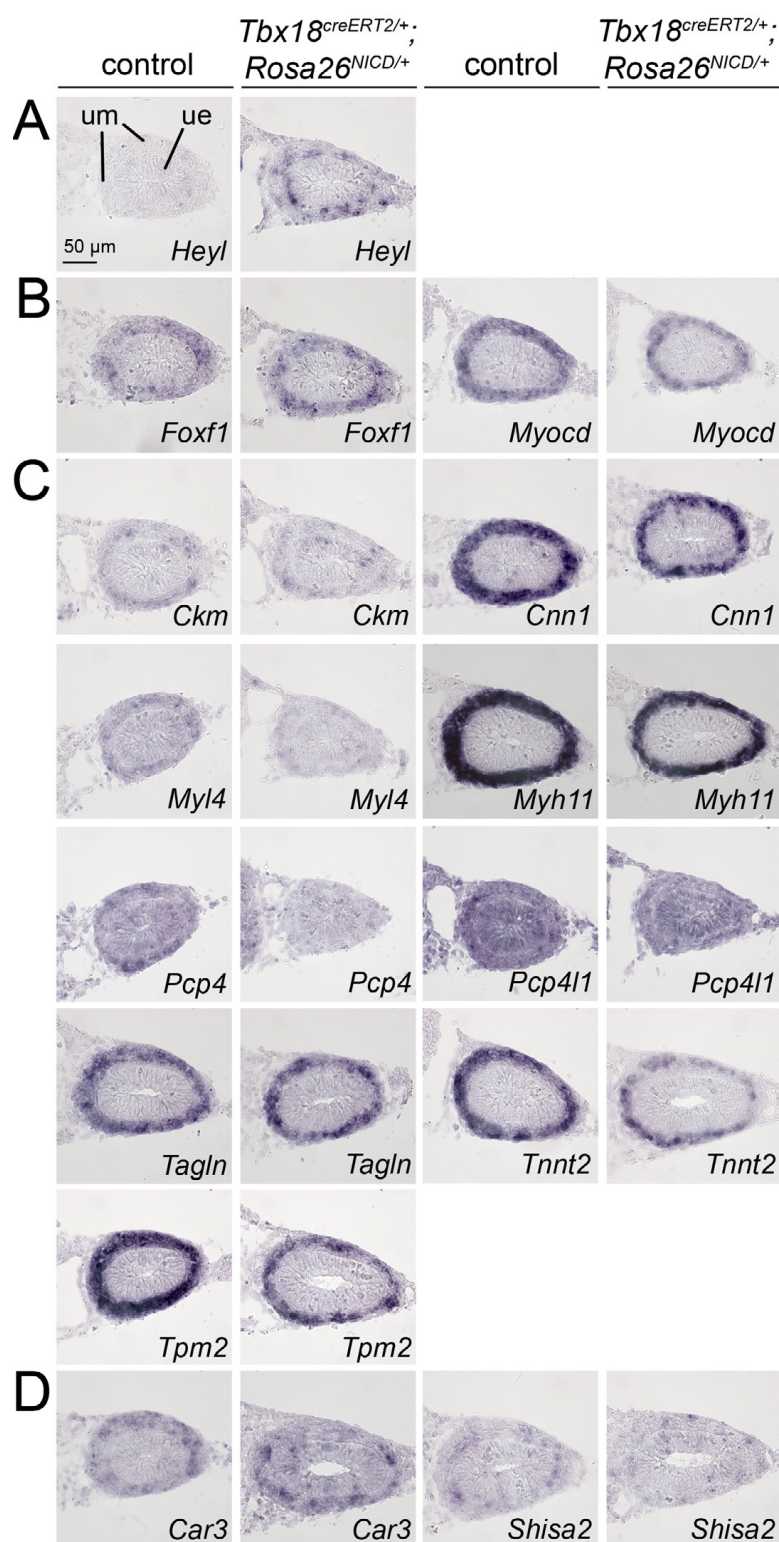


Fig. S13. Ectopic expression of the Notch1 intracellular domain (N1CD) affects the homogeneity of expression of SMC regulatory and structural genes in the UM. (A) RNA *in situ* hybridization analysis on transverse sections of organ explants of 13.5 control and *Tbx18*^{creERT2/+};*Rosa26*^{N1CD/+} ureters cultured for 4 days in the presence of 4-hydroxytamoxifen for expression of the Notch target gene *Heyl* (A), of SMC regulatory genes (B), of SMC structural genes (C), and of genes with reduced expression in the E14.5 *Rbpj*-cKO microarray, *Car3* and *Shisa2* (D); n=4 for all probes and genotypes. ue, ureteric epithelium; um, ureteric mesenchyme.

Table S1. Genes with altered expression in microarrays of E18.5 *Rbpj-cKO* ureters.

[Click here to download Table S1](#)

Table S2. Functional annotation and clustering of genes with decreased expression in E18.5 *Rbpk-cKO* ureters.

[Click here to download Table S2](#)

Table S3. Functional annotation and clustering of genes with increased expression in E18.5 *Rbpk-cKO* ureters.

[Click here to download Table S3](#)

Table S4. RT-qPCR analysis of expression of SMC genes in different conditions.

[Click here to download Table S4](#)

Table S5. Genes with altered expression in microarrays of P4 *Rbpj-cKO* ureters.

[Click here to download Table S5](#)

Table S6. Functional annotation of genes with decreased expression in the microarray of P4 *Rbpj-cKO* ureters.

[Click here to download Table S6](#)

Table S7. Functional annotation of genes with increased expression in the microarray of P4 *Rbpj-cKO* ureters.

[Click here to download Table S7](#)

Table S8. Functional annotation of genes with decreased expression in the microarrays of both E18.5 and P4 *Rbpj-cKO* ureters.

[Click here to download Table S8](#)

Table S9. Statistical analysis of contraction frequencies and intensities of E14.5 control and *Rbpj-cKO* ureters over 8 days of culture.

[Click here to download Table S9](#)

Table S10. Statistical analysis of contraction frequencies and intensities of E18.5 control and *Rbpj-cKO* ureters over 6 days of culture.

[Click here to download Table S10](#)

Table S11. Genes with altered expression in microarrays of E14.5 *Rbpj-cKO* ureters.

[Click here to download Table S11](#)

Table S12. Functional annotation of genes with altered expression in microarrays of E14.5 *Rbpj-cKO* ureters.

[Click here to download Table S12](#)

Table S13. Statistical analysis of ureter contraction frequency in contralateral explanted E12.5 ureters treated with either DMSO or 1 μ M DAPT or 2.5 μ M DAPT over 10 days of culture (relates to Figure 7A,B).

[Click here to download Table S13](#)

Table S14. Statistical analysis of ureter contraction frequency in contralateral explanted E18.5 ureters treated with either DMSO or 1 μ M DAPT over 6 days of culture (relates to Figure 7C).

[Click here to download Table S14](#)

Table S15. Statistical analysis of ureter contraction frequency in contralateral explanted P4 ureters treated with either DMSO or 1 μ M DAPT over 6 days of culture (relates to Figure 7E).

[Click here to download Table S15](#)

Table S16. Primer for RT-qPCR analysis of gene expression.

[Click here to download Table S16](#)